UNIVERSITY OF SPLIT

FACULTY OF ELECTRICAL ENGINEERING, MECHANICAL ENGINEERING AND NAVAL ARCHITECTURE

MECHANICAL ENGINEERING POSTGRADUATE STUDIES

DOCTORAL QUALIFYING EXAM

WATER AND HEAT MANAGEMENT FOR IMPROVED PERFORMANCE OF PROTON EXCHANGE MEMBRANE FUEL CELLS

Željko Penga

Split, January 2017

SVEUČILIŠTE U SPLITU

FAKULTET ELEKTROTEHNIKE, STROJARSTVA I BRODOGRADNJE

POSLIJEDIPLOMSKI DOKTORSKI STUDIJ STROJARSTVA

KVALIFIKACIJSKI ISPIT

UPRAVLJANJE VODOM I TOPLINOM U SVRHU POBOLJŠANJA RADNIH ZNAČAJKI MEMBRANSKOG GORIVNOG ČLANKA

Željko Penga

Split, siječanj 2017.

The doctoral qualifying exam was prepared at Department of mechanical engineering and naval architecture, Faculty of electrical engineering, mechanical engineering and naval architecture, Ruđera Boškovića 32, 21000 Split, Croatia.

Mentor: prof.dr.sc. Frano Barbir

Kvalifikacijski doktorski ispit je izrađen na Zavodu za strojarstvo i brodogradnju, Fakulteta elektrotehnike, strojarstva i brodogradnje, Ruđera Boškovića 32, 21000 Split, Hrvatska.

Mentor: prof.dr.sc. Frano Barbir

TABLE OF CONTENTS

LIST OF TABLES

There are no tables in this work.

LIST OF FIGURES

1 INTRODUCTION

Proton exchange membrane (PEM) fuel cells have gained a lot of attention in the recent years due to their favorable characteristics – simple design, high efficiency, low temperature, environmentally friendly operation due to virtually zero CO_2 emission and no moving parts [1-6]. They are also characterized by a wide range of application, from primary and auxiliary stationary applications to dynamic applications in road, sea and air vehicles.

However, the commonly used PEM fuel cell system is quite complex. The necessity for external temperature control of the cell via coolant loops and heat exchangers, and relative humidity control of the reactants upon entry to the cell results in high price and maintenance requirements for the system. The consequences are the requirement for an incubator-like setup for high efficiency PEM fuel cell system operation and limited operating range of the cell.

Limited operating range of PEM fuel cell system is a result of the requirement for external humidifiers. Since the ionomer membrane protonic conductivity is very sensitive to the net water transport balance through the membrane, i.e. to the water content of the membrane, the reactants need to have high relative humidity upon entering the cell to achieve high efficiency operation.

The idea of removing the external humidifiers is not new, however, there are only few commercial manufacturers who have managed to remove the external humidifiers with satisfactory cell performance, and the most advanced automotive fuel cell system without external humidification is commercially produced by Toyota [7]. However, Toyota uses hydrogen recirculation pump, which is also a costly component and has a similar function as the external humidifier, i.e. it recirculates the humidified hydrogen stream from the outlet back to the inlet to the cell. Therefore it can be concluded that complete removal of external humidification without compromising the high efficiency is not yet solved.

Since the number of works in the litarature on this topic are very few, this work is rooted on previous studies of Tolj et al. [8], but expands the mentioned work in meanings of studying different heat management strategies, since the mentioned work was based mostly on studying the water management and the temperature profiles along the cell. The external humidification in the mentioned work is completely removed, and the

performance of the cell is kept at a high level by prescribing a variable temperature flow field. The idea behind the mentioned, experimentally validated concept, is that the relative humidity of a gas is a temperature dependent parameter, and by manipulating the temperature across the entire flow field of the cell, one could impose such temperature profile which will result in close to 100% relative humidity along the entire cell for the specified amount of produced water inside the operating cell. However, the variable temperature flow field in the mentioned study is established by Peltier thermoelements, and it is only applicable for a simple single cell. This work investigates the possibility of establishing a variable temperature flow field by other means, feasible on a PEM fuel cell stack system level.

Useful tool for PEM fuel cell analysis which gaines more popularity in recent years is computational fluid dynamics (CFD) analysis. The CFD modeling enables generation of a virtual model of PEM fuel cell with all the relevant physical processes inside the operating cell. Until recently, CFD modeling was only possible on super computers, however, since the personal computers are advanced today, CFD modeling has become available to broad number of users. Once developed and validated, the CFD model can be used for different what-if scenarios, and give a detailed insight in complex physical processes inside an operating cell. However, since the models are based on experimentally derived expressions for different PEM fuel cell setups, and the experimental results of different authors show high degree of discrepancies, every CFD model must be experimentally calibrated and validated.

This work investigates literature recommendations for developing a CFD model which will enable the study of PEM fuel cell performance for different applied operating conditions and structural components. The goal of the CFD analysis is to develop a credible, i.e. experimentally validated, model where the desired temperature flow field will be established by a coolant liquid. The idea is to use internally generated heat to gradually increase the temperature of the coolant in the downstream direction in respect to the cell entry. The resulting temperature profile should closely resemble the desired temperature profile and the concept should be applicable for a PEM fuel cell stack. If such concept proves feasible, it will be the first of its kind, since no one up to date has been able to achieve it.

2 PROTON EXCHANGE MEMBRANE FUEL CELL

Proton exchange membrane fuel cell is electrochemical energy conversion device for converting the chemical energy of the reactants to electrical energy. It provides direct and continuous power output as long as the reactants are provided, and produces direct electrical current, with only byproducts being water and heat. The fuel for PEM fuel cells is hydrogen, in pure or in reformate form, and the oxydizer is pure oxygen or, more commonly, atmospheric air. The PEM fuel cell system does not have moving parts, and there is no combustion. The electrochemical process inside a PEM fuel cell is basically a reversed electrolysis of water, and, to a certain extent, similar to the process of galvanostatic electrochemical cell, i.e. battery, since it produces direct current electricity and consists of the anode and cathode with the electrolyte in between. The difference between galvanostatic cell and fuel cell is in the necessity of the fuel cell for constant reactant supply, therefore the fuel cell cannot be depleted, and the electrodes are not prone to rapid changes in chemical composition and they are covered by a thin layer of nano-particle platinum catalyst to improve the process of converting chemical to electrical energy.

There are different types of fuel cells, named after the type of the electrolyte, or fuel, used for operation. There are alkalyne, phosphoric acid, molten carbonate, solid oxide, polymer electrolyte or proton exchange membrane and direct methanol fuel cells. The main advantage of PEM when compared to other types of fuel cells is relatively low operating temperature (usually between 60°C and 80°C), high efficiency and the absence of aggressive chemical byproducts during operation.

2.1 Components

The components of PEM fuel cell are shown in Fig. 1.

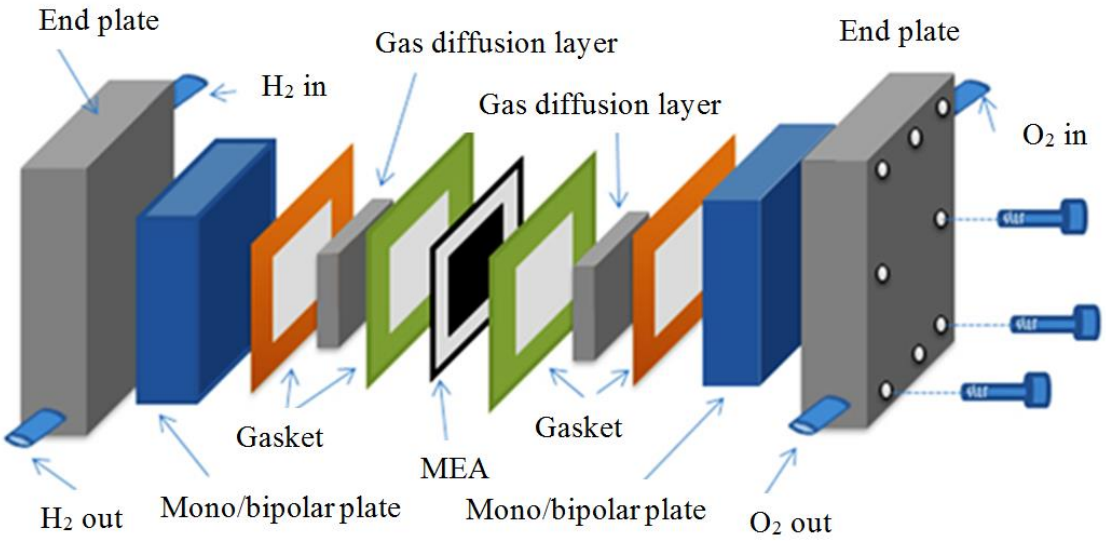

Figure 1. PEM fuel cell components – exploded view.

The PEM fuel cell components and their functions are:

- Polymer electrolyte or proton exchange membrane (perfluorosulfonated acid polymer, with the most commonly used from the international manufacturer DuPont under the name of Nafion®) ionomer membrane. This type of membrane allows free passage of cations, in PEM fuel cell case the hydrogen protons, but disables the passage of the gas molecules and electrons, hence the name proton exchange membrane.
- Catalys layer is a carbon supported structure coated with platinum nano-particles, it enhances the rate of the electrochemical reactions, without (intentional) change in composition over time. The catalyst layers are located on the anode and cathode side of the membrane.
- Membrane electrode assembly (MEA) consists of the membrane and catalyst layers on the anode and cathode side of the membrane, the MEA is usually provided by the manufacturer in the assembled form, hence the name.
- Gas diffusion layer is a porous structure made of carbon paper or carbon cloth, its primary function is to enable uniform reactant distribution along the entire flow field and removal of water generated inside the cathode catalyst layer. Gas diffusion layer is usually doped with polytetrafluorethylene to enhance the hydrophobicity, i.e. contact angle of water, on the gas diffusion layer surface.
- Bipolar plate is solid structure made from chemically inert materials which are relatively passive in the atmosphere of oxygen and hydrogen, commonly used materials are molded carbon (carbon powder impregnated with epoxy resin), stainless steel and

titanium. The function of bipolar plates is to enable supply of the reactants along the entire flow field via flow channels, i.e. flow field, machined or imprinted in the surface facing the membrane, to ensure structural requirements of the PEM fuel cell stack for the compression force applied, and to conduct electricity to the current collector terminals. Most of the commercial stacks also have a coolant loop, therefore the coolant channels are also machined between the adjacent bipolar plates. The coolant is used for heat removal from the stack and for maintenance of the desired temperature along the flow field. The name bipolar plate is derived from the fact that the anode side of one cell is serially connected to the cathode side of other cell. For a single cell, the bipolar plates can be referred to as monopolar plates.

- Gaskets are used to prevent reactant leakage during operation, and ensure uniform distribution of the pressure on the gas diffusion layers, the gaskets are placed between the bipolar plates around the membrane electrode assembly.
- End plate is a structural component of the cell to ensure the required uniform compression force along the entire flow field and keep the stack assembled during operation. End plates have specially designed fittings for the inlets and outlets of the reactants and the coolant. Some of the end plates have machined flow fields on the face in the membrane direction, in such cases they can be referred to as monopolar plates.

2.2 Operation principle and governing equations

Fuel cell is an energy conversion device that converts the chemical energy of fuel into electrical energy. Schematic of a PEMFC is shown in Fig. 2.

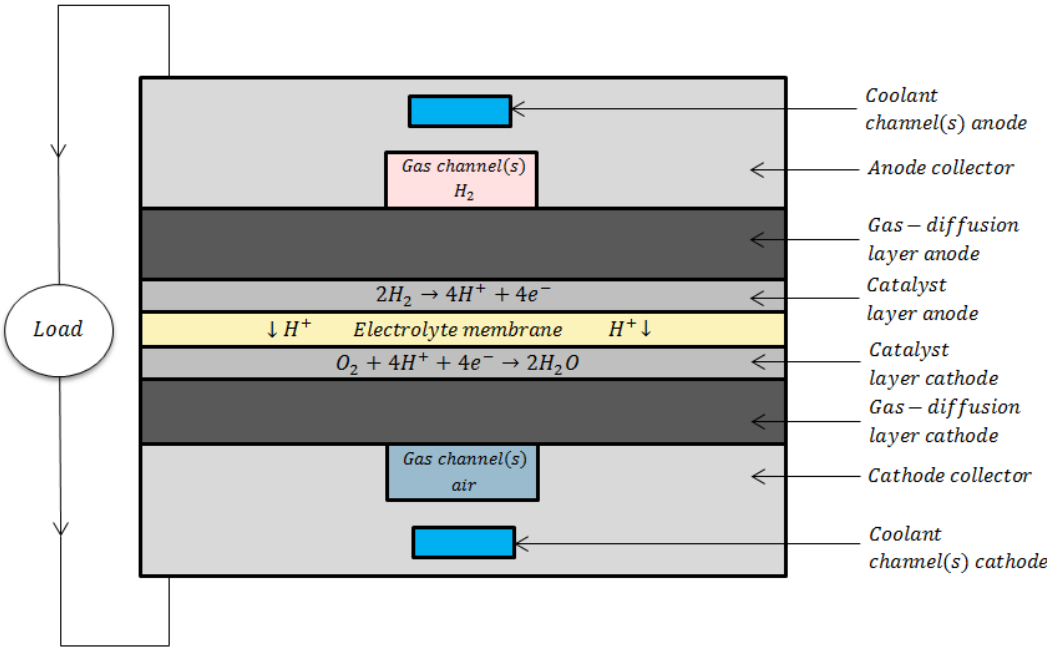

Figure 2. PEM fuel cell cut-through view.

This chapter is dedicated to description of the theoretical basis of PEM fuel cell modeling by using the computational fluid dynamics modeling software ANSYS Fluent®, along with brief description of the multi-physical phenomena inside an operating cell.

Hydrogen flows into the fuel cell on the anode side. It diffuses through the porous gas diffusion layers and reaches the catalyst layer, where it forms ions and electrons. The ions diffuse through the polymer electrolyte membrane, and electrons flow through the gas diffusion layer to the current collectors and into the electric load attached. The electrons enter the cathode side through the current collectors, and gas diffusion layer. Upon reaching the cathode catalyst layer, the electrons, hydrogen ions and oxygen combine to form water and release heat.

With ANSYS Fluent®, two electric potential fields are solved. One is solved in the electrolyte and the triple-phase boundary catalyst layer, while the other is solved in the triple-phase boundary catalyst layer, the porous electrode and the current collectors. The rates of electrochemical reactions are computed in the triple-phase boundary layers at both the anode and the cathode. Based on the cell voltage prescribed, the current density value

is computed – potentiostatic approach. Alternatively, the cell voltage can be computed based on a prescribed average current density – galvanostatic approach.

2.1.1 Overview

Over the last decade, the PEMFC has emerged as a favored technology for automotive trasportation and power generation due to its favorable characteristics: compact size, clean energy conversion, the ability to run at low temperatures (<100 °C), permition of of an adjustable power output, and the ability for a relatively rapid start.

Hydrogen is supplied at the anode, and air (or pure oxygen) is supplied at the cathode. The following chemical reactions take place in the anode and cathode triple-phase boundaries, respectively

$$H_2 \Leftrightarrow 2H^+ + 2e^- \text{ (anode)} \quad (1)$$

$$\frac{1}{2}O_2 + 2e^- + 2H^+ \Leftrightarrow H_2O \text{ (cathode)} \quad (2)$$

Electrons produced in the anode travel through an external circuit to the cathode, while protons (H^+) travel through the membrane from the anode triple-phase boundary to the cathode triple-phase boundary, thereby forming an electrical circuit.

As the amount of generated water increases at the cathode, due to the effect of osmotic drag and electrochemical reactions, water vapor pressure exceeds the saturation pressure and liquid water is formed. The occurence of liquid water in the cathode can strongly influence the performance of PEMFC.

2.1.2 Electrochemistry

The electrochemistry modeling is revolved around the computation of the rates of the anodic and cathodic reactions. The electrochemistry model adopted in ANSYS Fluent is the one used by other groups [9-11].

The driving force behind the reactions is the surface overpotential – the difference between the phase potential of the solid and the phase potential of the electrolyte/membrane. For this reason, two potential equations are solved within Fuel Cell Module. One potential equation (3) accounts for the electron e^-transport through the solid conductive materials – current collectors and solid portion of the porous media, while the other potential equation (4) represents the ionic transport of H^+ or O^{-2}. The two potential equations are

$$\nabla(\sigma_{sol}\nabla\phi_{sol}) + R_{sol} = 0 \quad (3)$$

$$\nabla(\sigma_{mem}\nabla\phi_{mem}) + R_{mem} = 0 \quad (4)$$

where σ ($\Omega^{-1}m^{-1}$) represents electrical conductivity, ϕ (V)is electric potential and R (Am^{-3}) represents volumetric transfer current.

There are two types of external boundary conditions: those that allow the passage of electrical current, and those that do not. Fig. 3. Illustrates the boundary conditions used for solving ϕ_{sol} and ϕ_{mem}.

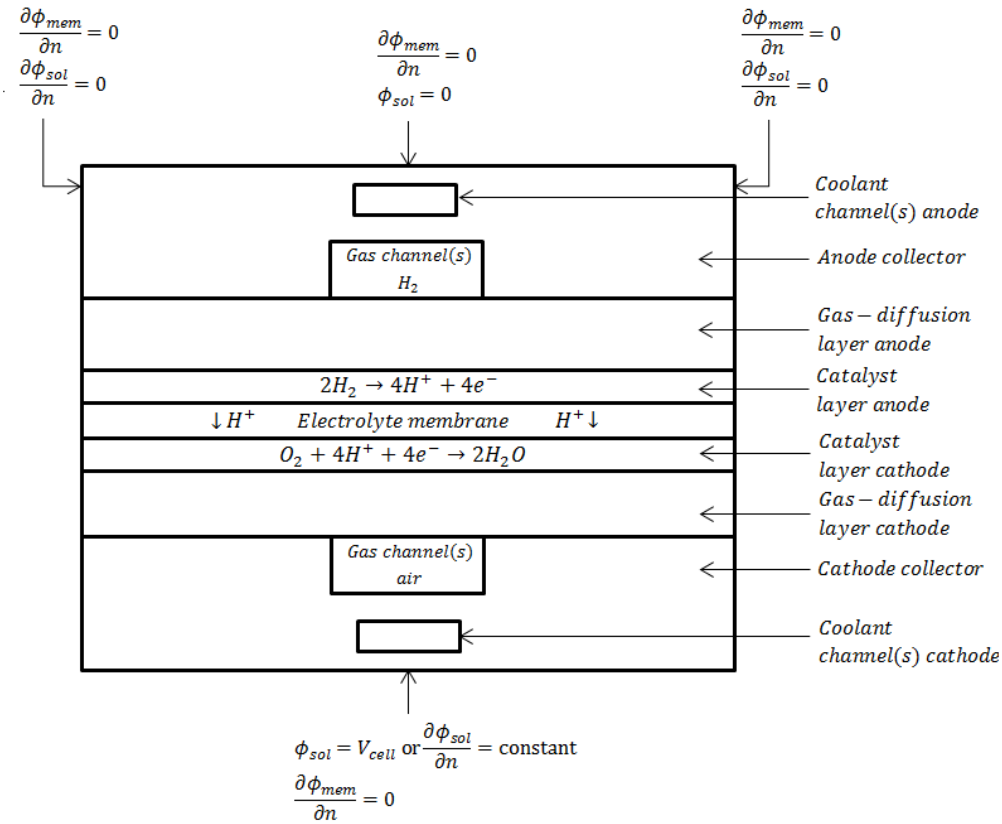

Figure 3. External electrical boundary conditions.

Since ionic current does not leave the fuel cell through external boundaries, all external boundaries have a zero flux boundary condition for the membrane phase potential ϕ_{mem}. For the solid phase potential ϕ_{sol}, the external boundaries on the anode and the cathode side are in contact with the external electric circuit and the electrical current generated by the fuel cell passes only through these boundaries, *i.e.* current collector terminals. All other external boundaries are defined as zero flux boundary conditions for ϕ_{sol}.

The external boundaries can be defined in two ways. Both ways require definition of zero electric potential on the anode side. The first way is definition of a positive value of electric potential on the cathode terminals, *i.e.* potentiostatic approach. The second is definition of a negative value of current flux density on the cathode terminals (in Am^{-2}). The first approach is recommended by the manual [12], but since the resulting current density is unknown in the first iteration, it requires a couple of steps to get the desired current density for a fixed mass flow rate. The first approach enables definition of the desired electric potential regardless of its value. The second approach is straight-forward, since the mass flow rate of the reactants is easily determined, but it requires application of a smaller current density in the beginning and step-like increase of the current flux density with a maximal step of 0.2 Acm^{-2} to get to the desired current density, or the solution will diverge.

The transfer currents, *i.e.* the source terms from equations 3 and 4, are non-zero only inside the catalyst layers and are computed as:

For the solid phase, $R_{sol} = -R_{an} (< 0)$ on the anode side and $R_{sol} = +R_{cat} (> 0)$ on the cathode side

For the membrane phase, $R_{mem} = +R_{an} (> 0)$ on the anode side and $R_{mem} = -R_{cat} (< 0)$ on the cathode side

The source terms R_{an} and R_{cat} in equations 3 and 4 are also called the exchange current densities (Am^{-3}), the general definitions of exchange current densities are

$$R_{an} = \left(\zeta_{an} j_{an}^{ref}\right)\left(\frac{[A]}{[A]_{ref}}\right)^{\gamma_{an}} \left(e^{\frac{\alpha_{an} F \eta_{an}}{RT}} - e^{\frac{-\alpha_{cat} F \eta_{an}}{RT}}\right) \tag{5}$$

$$R_{cat} = \left(\zeta_{cat} j_{cat}^{ref}\right)\left(\frac{[C]}{[C]_{ref}}\right)^{\gamma_{cat}} \left(-e^{\frac{\alpha_{an} F \eta_{cat}}{RT}} + e^{\frac{-\alpha_{cat} F \eta_{cat}}{RT}}\right) \tag{6}$$

where j^{ref} represents exchange current density per active surface area, ζ specific active surface area, $[\,], [\,]_{ref}$ local species concentration, γ concentration dependency coefficient, α transfer coefficient, F Faraday constant, η local overpotential, *i.e.* activation loss, R gas constant and T temperature. Equations (5) and (6) represent the general formulation of the Butler-Volmer function. A simplified form of the expression is given in the form of Tafel formulation

$$R_{an} = \left(\zeta_{an} j_{an}^{ref}\right)\left(\frac{[A]}{[A]_{ref}}\right)^{\gamma_{an}} \left(e^{\frac{\alpha_{an} F \eta_{an}}{RT}}\right) \quad (7)$$

$$R_{cat} = \left(\zeta_{cat} j_{cat}^{ref}\right)\left(\frac{[C]}{[C]_{ref}}\right)^{\gamma_{cat}} \left(e^{\frac{-\alpha_{cat} F \eta_{cat}}{RT}}\right) \quad (8)$$

By default, the Butler-Volmer function is used inside the ANSYS Fluent Fuel Cell Module for computation of transfer currents inside the catalyst layers. In equations (5–8), $[A]$ and $[C]$ represent the molar concentration of the species upon which the anode and cathode reaction rates depend, recpectively. For PEMFC, A represents H_2 and C represents O_2.

The driving force for the kinetics is the local surface overpotential η, known as the activation loss, and it generally represents the difference between the solid ϕ_{sol} and membrane ϕ_{mem} potentials. The gain in electric potential from crossing from the anode to the cathode side is taken into account by subtracting the open-circuit voltage V_{OC} on the cathode side

$$\eta_{an} = \phi_{sol} - \phi_{mem} \quad (9)$$

$$\eta_{cat} = \phi_{sol} - \phi_{mem} - V_{OC} \quad (10)$$

Equations 3-10 are used for obtaining the two potential fields.

2.1.3 Current and mass conservation

Species volumetric source terms in the triple-phase boundaries due to electrochemical reactions for the PEMFC are

$$S_{H_2} = -\frac{M_{w,H_2}}{2F} R_{an} < 0 \quad (11)$$

$$S_{O_2} = -\frac{M_{w,H_2}}{4F} R_{cat} < 0 \quad (12)$$

$$S_{H_2O} = \frac{M_{w,H_2O}}{2F} R_{cat} > 0 \quad (13)$$

Since the total electrical current produced in the cathode and the anode triple-phase boundaries is the same, the following equation is considered for current conservation

$$\int_{an} R_{an} dV = \int_{cat} R_{cat} dV \quad (14)$$

2.1.4 Heat source

Additional volumetric sources to the thermal energy equation are present because not all chemical energy released in the electrochemical reactions can be converted to electrical work due to irreversibility of the processes. The total source that sums up the energy equation, *i.e.* enthalpy is

$$S_h = h_{react} - R_{an,cat}\eta_{an,cat} + I^2 R_{ohm} + h_L \tag{15}$$

where h_{react} represents the net enthalpy change due to the electrochemical reactions, $R_{an,cat}\eta_{an,cat}$ the product of the transfer current and overpotential in the anode or cathode triple-phase boundaries, R_{ohm} the ohmic resistance of the conducting media, and h_L is the enthalpy change due to condensation/vaporization of water.

2.1.5 Liquid water formation, transport and its effects

Since PEMFCs operate under relatively low temperatures (<100 °C), the water vapor may condense to liquid water, especially at high current densities. While the existence of the liquid water keeps the membrane hydrated, it also prevents the gas diffusion, reduces the diffusion rate and the effective reacting surface area and consequently the cell performance. To model the formation and transport of liquid water, ANSYS Fluent uses a saturation model based on [13,14]. In this approach, the liquid water formation and transport is governed by the following conservation equation for the volume fraction of liquid water, s, or the water saturation

$$\frac{\partial(\varepsilon\rho_l s)}{\partial t} + \nabla(\rho_l \vec{v}_l s) = r_w \tag{16}$$

where the subscript l stands for liquid water, and r_w is the condensation rate that is modeled as

$$r_w = c_r \max\left(\left[(1-s)\frac{p_{wv} - p_{sat}}{RT}\, M_{w,H_2O}\right], [-s\rho_l]\right) \tag{17}$$

where $-r_w$ is added to the water vapor equation, as well as the pressure correction (mass source). This term is applied only inside the catalyst and gas diffusion layers. The condensation rate constant is hardwired to $c_r = 100\ s^{-1}$. It is assumed that the liquid velocity v_l is equivalent to the gas velocity inside the gas channel (that is, a fine mist).

Inside the highly-resistant porous zones, the use of the capillary diffusion term allows us to replace the convective term in equation (16), with

$$\frac{\partial(\varepsilon\rho_l s)}{\partial t} + \nabla\left[\rho_l \frac{Ks^3 dp_c}{\mu_l ds}\nabla s\right] = r_w \tag{18}$$

Depending on the wetting phase, the capillary pressure is computed as a function of s (the Leverett function)

$$p_c = \begin{cases} \dfrac{\sigma cos\theta}{\left(\frac{K}{\varepsilon}\right)^{0.5}}(1.417(1-s) - 2.12(1-s)^2 + 1.263(1-s)^3) & \theta_c < 90° \end{cases} \tag{19}$$

$$\begin{cases} \dfrac{\sigma cos\theta}{\left(\frac{K}{\varepsilon}\right)^{0.5}}(1.417s - 2.12s^2 + 1.263s^3) & \theta_c > 90° \end{cases} \tag{20}$$

where ε represents the porosity, σ the surface tension, θ_c the contact angle and K the absolute permeability. Equation (16) is used for modeling various physical processes, such as condensation, vaporization, capillary diffusion and surface tension. The clogging of the porous media and the flooding of the reaction surface are modeled by multiplying the porosity and the active surface area by $(1-s)$, respectively.

2.2 Physical properties and water transport through the membrane

The following expressions are used for calculation of the physical properties of materials and the water transport across the membrane.

2.2.1 Gas phase species diffusivity

Gas phase species diffusivities can be computed either by using the dilute approximation method, or by using the full multicomponent method. The dilute approximation method is represented by

$$D_i = \varepsilon^{1.5}(1-s)^{r_s} D_i^0 \left(\frac{p_0}{p}\right)^{\gamma_p}\left(\frac{T}{T_0}\right)^{\gamma_t} \tag{21}$$

where D_i^0 represents the mass diffusivity of species i at reference temperature and pressure p_0, T_0 (reference 9). The reference values and the exponents, γ_p, γ_t, as well as the exponent of pore blockage r_s are defined in the Fluent Fuel Cell Module® user defined functions as

$$p_0 = 101325 \text{ Nm}^{-2} \quad (22)$$
$$T_0 = 300 \text{ K}$$
$$\gamma_p = 1$$
$$\gamma_t = 1.5$$
$$r_s = 2.5$$

In addition to equation 20, the Fluent Fuel Cell Module® also contains a method for computation of the gas phase species diffusion, *i.e.* a full multicomponent diffusion method with correction for the porous media tortuosity

$$D_{eff}^{ij} = \varepsilon^{1.5} D^{ij} \quad (23)$$

where D_{eff}^{ij} represents the effective gas species diffusivity, ε porosity of the porous medium, and D^{ij} is the gas species mass diffusivity computed by the full multicomponent diffusion method. Properties such as electrolyte phase electrical conductivity, water diffusivity and osmotic drag coefficient are evaluated as functions of the water content, using correlations as suggested by [15]. To capture the relevant physics of the problem, various properties of the membrane are incorporated into the model as default options.

2.2.2 Electrolyte phase (ionic) conductivity

For PEMFC, the electrolyte (membrane) phase conductivity is modeled as

$$\sigma_{mem} = \beta(0.514\lambda - 0.326)^{\omega} e^{1268(\frac{1}{303} - \frac{1}{T})} \quad (24)$$

where λ represents the membrane water content. The constants β and ω are introduced in ANSYS Fluent for generality. Equation (24) becomes the original correlation from [15] when $\beta = \omega = 1$.

2.2.3 Osmotic drag coefficient

$$n_d = \frac{2.5\lambda}{22} \quad (25)$$

2.2.4 Back diffusion flux

$$J_w^{diff} = -\frac{\rho_m}{M_m} M_{H_2O} D_l \nabla\lambda \quad (26)$$

where ρ_m and M_m represent the density and equivalent weight of the dry membrane, respectively, and D_l is membrane water diffusivity.

2.2.5 Membrane water diffusivity

$$D_l = 3.1 \times 10^{-7}\lambda\left(e^{0.28\lambda} - 1\right)\left(e^{-\frac{2346\ [\mathrm{K}]}{T}}\right) \quad \lambda < 3 \tag{27}$$

$$D_l = 4.17e \times 10^{-8}\lambda\left(1 + 161e^{-\lambda}\right)\left(e^{-\frac{2346\ [\mathrm{K}]}{T}}\right) \quad \lambda \geq 3$$

2.2.6 Membrane water content

The expression for the membrane water content λ is obtained using Springer et al. correlation [15].

$$\lambda = 0.043 + 17.18a - 39.85a^2 + 36a^3 \quad a < 1 \tag{28}$$

$$\lambda = 14 + 1.4(a - 1) \quad a \geq 1$$

where a represents the water activity, defined as

$$a = \frac{p_{wv}}{p_{sat}} + 2s \tag{29}$$

2.2.7 Water vapor pressure

The water vapor pressure is computed from the vapor molar fraction x and the local pressure p

$$p_{wv} = x_{H_2O}p \tag{30}$$

2.2.8 Saturation pressure

The default unit for saturation pressure calculation in ANSYS Fluent is atm, defined by the following expression

$$\log_{10} p_{sat} = -2.1794 + 0.02953(T - 273.17) \tag{31}$$

$$-9.1837 \times 10^{-5}(T - 273.17)^2$$

$$+1.4454 \times 10^{-7}(T - 273.17)^3$$

It is noted here that in [15], water activity is defined on the basis of total water or super-saturated water vapor. With phase change being invoked in the present two-phase model, $2s$ is added to the original formulation as suggested by [16].

2.3 Leakage current (cross-over current)

The leakage current, I_{leak}, models the effect of species cross-over from one electrode to another across the electrolyte. In addition to the source terms expressed by equations (11–13), the expressions are

$$S_{H_2} = -\frac{M_{w,H_2}}{2F \cdot Vol_{anode}} I_{leak} \tag{32}$$

$$S_{O_2} = -\frac{M_{w,O_2}}{4F \cdot Vol_{cathode}} I_{leak} \tag{33}$$

$$S_{H_2} = -\frac{M_{w,H_2O}}{2F \cdot Vol_{anode}} I_{leak} \tag{34}$$

2.4 Fluid dynamics

2.4.1 Continuity

$$\nabla(\rho \vec{V}) = S_{mass} \tag{1}$$

where S_{mass} represents source term for continuity equation. This term is only applicable for the triple-phase boundary (catalyst) regions. Inside the gas channels, gas diffusion layers and the membrane, the source term S_{mass} is set to zero.

2.4.2 Momentum

$$\frac{1}{s(1-s)}\nabla(\rho \vec{V}\vec{V}) = -\nabla p + \frac{1}{s(1-s)}\nabla(\mu \nabla \vec{V}) + \rho g + S_{mom} \tag{2}$$

where S_{mom} represents the source term for momentum equation and applies only for the porous medium. For other domains, S_{mom} is set to zero.

2.4.3 Species

$$\nabla(\rho \vec{V} X_i) = -\nabla(\rho D_i \nabla X_i) + S_i \tag{3}$$

where the index *i* represents different species – oxygen, hydrogen and water vapor. The term S_i represents the source and sink term for the species inside the catalyst layers and accounts for the reactant consumption in anode and cathode catalyst layers and water generation inside the cathode catalyst layer. In other domains, the term S_i value is set to zero.

2.4.4 Energy

$$\nabla\left(\rho\,\vec{V}T\right) = \nabla(k^{eff}\nabla T) + S_T \tag{4}$$

where S_T represents the heat source term for the energy equation. The heat source term S_T applies only for the cathode catalyst layer, for other domains it is set to zero.

3 REVIEW OF PREVIOUS RESEARCH

PEM fuel cell operation is highly dependent on water and heat management [8,17]. The water management is important because the membrane ionic conductivity is proportional to the membrane water content, i.e. number of water molecules per one perfluorosulfonic acid molecule [18], as previously mentioned. The membrane water content is dependent on relative humidity of the reactants. If relative humidity of the reactants is low, the membrane will be dehydrated, and the ionic conductivity of the membrane will be low, therefore high relative humidity of the reactants is required for high performance operation. To ensure high relative humidity of the reactants, the reactants require humidification before entering the cell. The necessity for external humidification increases the system complexity and economic costs. Humidification is a thermodynamic process based on evaporating liquid water and saturating the reactant gas passing through the humidifier with water vapor at 100% relative humidity for the prescribed temperature, therefore the process requires water and heat. Since water and heat are already produced during PEM fuel cell operation from the electrochemical reaction of hydrogen and oxygen on the triple-phase boundaries inside the cathode catalyst layer, it is logical to presume that the generated water and heat could be used to humidify the reactants and thereby improve the performance of the cell [1,17,19]. The generation of liquid water is especially important at higher current densities, since the reactants are already saturated with water vapor, and cannot evaporate the generated water. This results in pooling of the liquid water inside the porous gas diffusion layers and decreases the active area of the catalyst layers since the reactants are unable to pass through liquid water. Excessive water accumulation in the gas diffusion layers can cause the flooding of the reactant channels and consequently cause starvation of the cell. Starvation of the cell results in catastrophic performance and irreversible degradation of the cell [17] and must therefore be prevented at all times.

The relative humidity of the reactants, fuel (hydrogen) and oxidant (pure oxygen or oxygen from atmospheric air) is one of the most important operating parameters of PEM fuel cell [1]. There are many works dealing with investigation of the influence of relative humidity of the reactants on PEM fuel cell operation and efficiency [19-24]. The idea of keeping the relative humidity of the reactants along the entire flow field near the water vapor saturation profile is beneficial for the cell operation and results in increased life time of the cell. However, as previously mentioned, the water balance of the cell is a very sensitive topic since it affects the membrane ionic conductivity. The flooding results in

unstable polarization curve, while higher amounts of liquid water inside the cell cause mass transport losses, evident from sudden decrease in operating electric potential at higher operating current densities. Operation in membrane dehydration regimes, or cycling between low and high relative humidity of the reactants results in increased degradation of the cell [25].

Heat management of PEM fuel cell is important due to the fact that the relative humidity of reactants is temperature dependent, since the pressure drop is minor. The cell is usually kept at a constant temperature along the entire flow field and regulated with the coolant fluid mass flow rate. The coolant enters the cell at a prescribed temperature with the mass flow rate which will result in uniform temperature distribution (i.e. very small temperature gradient) along the entire flow field. However, since the fuel cell generates heat during operation, the coolant temperature will increase towards the outlet of the cell. If the bipolar plates are made from materials characterized by low thermal conductivity, the temperature along the reactant channels will be higher than the temperature of the coolant liquid. For the same amount of generated water, i.e. for the same generated electrical current, the result is decreased relative humidity of the reactants, and decreased performance of the cell, i.e. decreased electric potential. Therefore, special care must be taken to account for this temperature difference.

Besides water and heat management, there are other parameters influencing PEM fuel cell operation, such as the flow field geometry, i.e. the shape and size of the reactant channels, the clamping force (which is usually prescribed by the manufacturer of the membrane electrode assembly, but not in all cases), temperature and gauge pressure of the reactants, and the microstructure of the membrane, electrodes and the porous gas diffusion layers. One of the most comprehensive approaches for investigating in situ operation of the cell is segmentation of the fuel cell [1,8,26-31]. The segmentation of the cell is basically division of a single cell in a number of electrically and thermally insulated segments, and enables measurement of the operating parameters such as electrical current, temperature and sometimes even relative humidity before and after each segment of the cell. The segments are electrically interconnected in parallel with a common current collector terminal. This enables investigation of the condensation of water inside the cell during operation, the membrane dehydration, and water transport (if relative humidity is measured before and after each segment). It also enables the study of the current density distribution

along the cell, and investigation of the rate of change of operating parameters under dynamic load changes, which is of special importance for automotive applications.

Experimental segmented fuel cell can be used for determination of the optimal operating parameters of the cell and enable development of a robust numerical model which can be later used for different what-if scenarios to determine the parameter sets for high performance of the cell.

The following chapters give insight in the research by different groups of authors in the fields of heat [32-37] and water management of PEM fuel cells [38-48], computational fluid dynamics modeling [49-55] of PEM fuel cells and the design of an advanced model of a segmented PEM fuel cell [8,26] required for in-depth experimental investigation.

3.1 Heat management

Heat management of PEM fuel cells represents the balance of the generated heat by the electrochemical reactions of hydrogen and oxygen inside an operating cell with the adequate methods of heat removal from the system. Most of the research done by different groups of authors in the past is concentrated on establishing a uniform temperature flow field for PEM fuel cell operation, however, some of them indicated the potential of improving the performance of the fuel cell by introducing a spatially variable temperature flow field.

Zhang and Kandlikar [32] investigated the applicability of different coolant strategies for PEM fuel cell stacks. The investigated coolant techniques were (i) cooling with heat spreaders, i.e. passive cooling, (ii) cooling with separate air flow, (iii) cooling with liquid coolant (water or propylene-glycol and water mixture), and (iv) evaporation cooling, i.e. cooling through boiling. The conclusion is that (i) heat spreader cooling requires very expensive materials such as pyrolytic graphite, characterized by extremely high in-plane thermal conductivities to enable sufficient heat dissipation at higher operating loads. Cooling with separate air flow (ii) is inefficient due to very low specific heat of air, and the requirement for high mass flow rates of air in the separate cooling channels, resulting in requirement for higher overall volume of the stack and only applicable for lower operating current densities. Liquid cooling (iii) is observed to have the most applicability due to the fact that water has very high specific heat and enables sufficient heat removal rates even at high currents, while the propylene-glycol and water mixture enables operation for sub-zero start-up temperatures. The problem with liquid

cooling is ionization of the coolant water with operation, and in order to prevent this behavior the water must be deionized after a certain electrical conductivity is reached. This can be prevented by using kerosene instead of water, with roughly half the specific heat of water and required twice higher mass flow rate, but does not require de-ionization during operation of the cell. The problem with liquid cooling is the requirement for a circulation pump, heat exchanger and the temperature control of the coolant water. Evaporation cooling (iv) is an interesting solution for PEM fuel cell cooling, however, it does not enable sufficient cooling of the cell, since the evaporative cooling can roughly dissipate only 10-15% of the required heat for high performance of the cell. Evaporative cooling can however improve the performance of the cell during operation when coupled with liquid cooling. The general conclusions of this work are that the liquid cooling is the only option for higher current densities and PEM fuel cell stack cooling.

Chen et al. [33] investigated the influence of different coolant flow fields on fuel cell performance, in order to optimize the coolant flow field configuration for a PEM fuel cell stack. The criterion for cooling efficiency was the overall temperature variation along the entire area of the cooling flow field, by the self-proclaimed Index of Uniform Temperature. Six different flow fields were investigated and compared, three of the serpentine configuration and three of a parallel configuration, Fig. 4. Serpentine coolant flow field resulted in higher Index of Uniform Temperature, meaning that the overall temperature difference was lower when compared to the parallel coolant flow field, however the pressure drop across the serpentine flow field is higher. However, the influence of the temperature non-uniformity on the cell performance was not studied in this work.

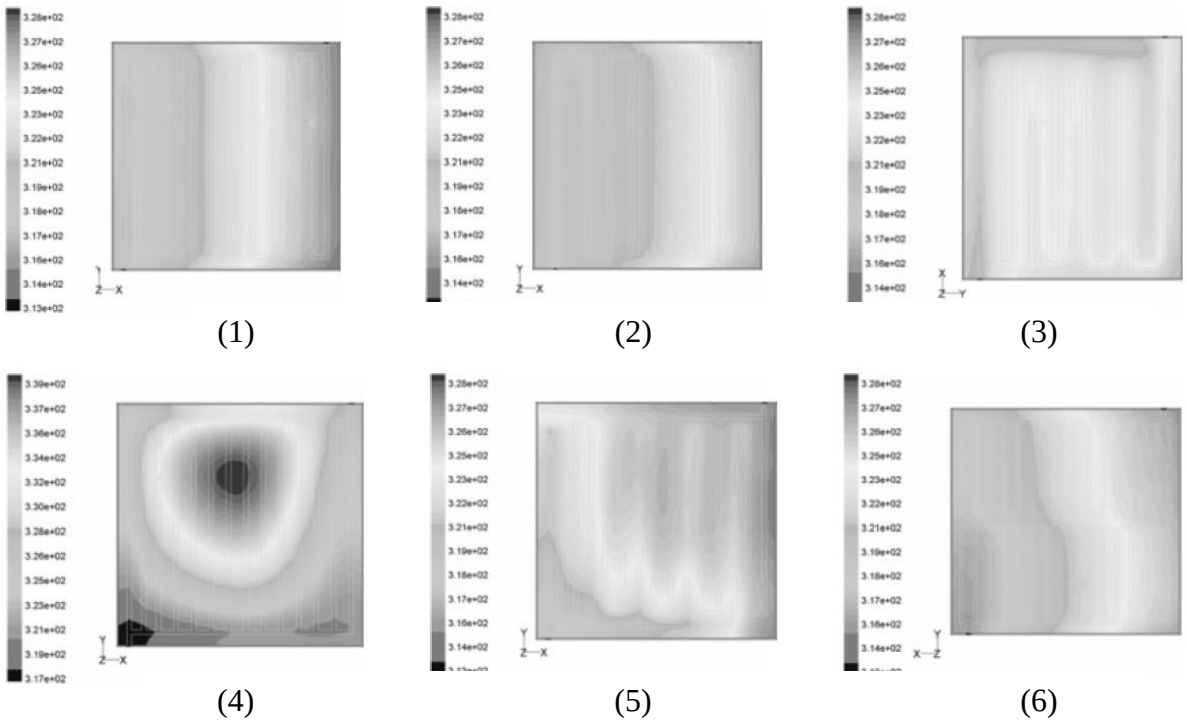

Figure 4. Comparison of temperature distributions along the current collectors for serpentine (1,2,3), and parallel (4,5,6) flow field configurations, adopted from [33].

Mench et al. [34] have proposed that non-uniform cooling could be beneficial for PEM fuel cell performance if optimized for the prescribed reactant gas flow rates and operating parameter configuration. If the coolant channels are designed and flow rates are such that the temperature in the gas channels gradually increases in the downstream direction, it can be used to mitigate the flooding issue, since the water saturation pressure is increasing with the temperature. The concept of non-uniform, i.e. variable, cooling in this work was only proposed on a theoretical basis, and was not tested experimentally.

Wilkinson et al. [35] patented a stack with co-flow configuration of the coolant with the cathode air, while the anode hydrogen was in counter-flow configuration in respect to the coolant and cathode air. Such setup led to non-uniform cooling, as previously theorized by Mench et al. [34]. The experiments were carried out on a 4-cell stack and the performance of the stack was superior for each temperature differential tested (5, 10, 15 and 20°C) compared to the co-flow of reactants with the coolant. However, this work did not determine the optimal temperature profile, but it resulted in credibility of the non-uniform temperature flow field concept for further investigation.

Kang et al. [36] numerically investigated the influence of the anode, cathode and coolant flow field configurations on the performance of PEM fuel cell. The conclusion was

that the counter flow configuration of air and hydrogen, and co-flow of air and coolant result in the highest cell performance, as previously seen in an experimental study of Wilkinson et al. [35]. The performance gain was attributed to higher membrane hydration in the reported configuration. Conclusion of this work was that the experimental data is also successfully modeled and validated by using the numerical approach, but further insight in the physical meaning of the non-uniform temperature profile on PEM fuel cell performance was not clear.

Tolj et al. [8] investigated the PEM fuel cell performance for non-uniform temperature flow field prescribed along the cathode flow field by means of Peltier thermoelements. The single cell was divided in five equal parts, and the temperature profile was extracted from Mollier's h-x chart to closely resemble the water saturation profile, i.e. to achieve relative humidity close to 100% along the entire flow field, Fig. 5.

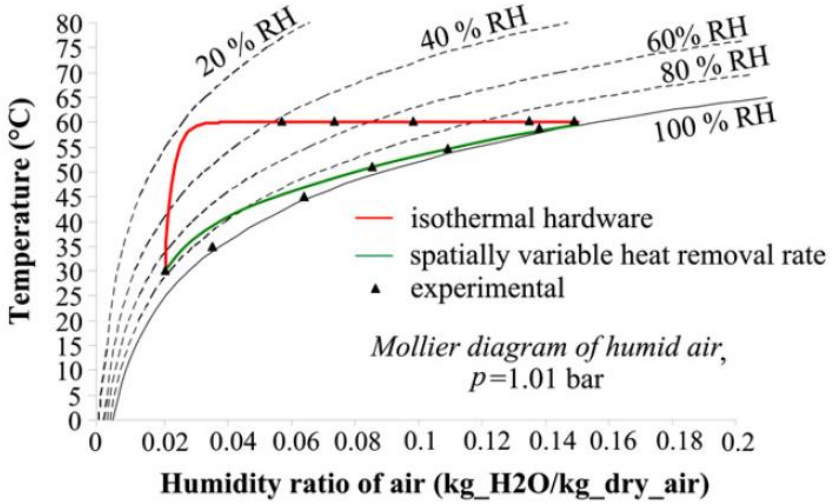

Figure 5. Humidification of air stream along the cathode channel in Mollier's *h-x* chart, isothermal vs. spatially variable heat removal rate (non-uniform temperature flow field), adopted from [8].

The cell was fed with dry hydrogen and ambient condition air. The experimental results have shown significant improvement in performance when compared to the isothermal case, especially for higher current densities. Establishment of close to 100% relative humidity along the entire flow field resulted in minimized mass transport losses, a consequence of evaporating the generated liquid water. The relative humidity was measured before and after each segment, and good agreement is achieved with a simple pseudo 2-D model which was also developed in the mentioned work. However, the anode

side relative humidity was not measured. Therefore there was no insight in the water transport through the membrane, since it is not possible to determine the balance between the electro-osmotic drag and the back-diffusion flux through the membrane. The requirement for Peltier thermoelements results in non-applicability of the concept for commercial PEM fuel cell stacks.

Ozden et al. [37] developed a three-dimensional computational fluid dynamics numerical model for the experimental setup from Tolj et al. [8]. The single cell was designed with spatially variable heat removal rates, in order to establish the desired temperature profile resulting in close to 100% relative humidity along the entire flow field. The spatially variable heat removal was achieved by introducing aluminum ribs on the cathode side. This work has shown that it is possible to numerically model the non-uniform temperature flow field. However, the relative humidity profile on the cathode side was quite different from the results obtained by Tolj et al. [8] even though it had a similar shape. The concept of using passive cooling was already deemed inefficient for PEM fuel cell stack, as mentioned previously in the work of Zhang and Kandlikar [32], therefore a more robust method of cooling the stack with non-uniform temperature distribution is required.

3.1.1 Conclusions

Investigation of the research by other authors in the field of heat management of PEM fuel cells results in the conclusion that the only feasible cooling system for PEM fuel cell stacks is liquid cooling, which can be used to establish a non-uniform temperature profile along the entire flow field. The coolant channels should be parallel, since they result in non-uniform temperature flow field by default and lower pressure drop when compared to the serpentine flow field. The resulting temperature profile along the flow field should closely resemble the water vapor saturation profile, since the water vapor saturation pressure is temperature dependent. The flow field setup should have cathode air in counter-flow configuration with the anode hydrogen, while the coolant flow should be in co-flow configuration with the cathode air, since the result is better overall hydration of the membrane. The required temperature profile for high performance PEM fuel cell operation, i.e. water vapor saturation temperature profile, without the requirement for external humidification can be extracted from Mollier's *h-x* chart, based on calculating the amount of generated water inside the cell and the initial conditions of the reactant gases, i.e. temperature and relative humidity of the air and hydrogen upon entry to the cell. It

would be very useful to develop a three-dimensional computational fluid dynamics model in order to investigate the cell for different operating conditions. The computational fluid dynamics model should first be calibrated with experimental results for a fixed temperature profile established on the current collector terminals via Peltier thermoelements, and later the temperature profile could be established by the coolant mass flow rate control. The result would be PEM fuel cell setup applicable for commercial stack applications, without the requirement for external humidification.

3.2 Water management

Water management of PEM fuel cells dictates the performance of the cell. The ionic conductivity of the membrane of PEM fuel cell is highly dependent on the membrane water content. If the membrane is dry, the ionic conductivity is low, resulting in poor performance due to high ohmic losses and increased degradation rates. High membrane hydration, resulting from the common application of the external humidification of the reactants, can result in the flooding of the catalyst layers, the gas diffusion layer and the channels at higher current densities, causing a sudden decrease of the cell performance and non-uniform reactant and temperature distribution inside an operating cell, i.e. high mass transport losses. Such operation also results in increased degradation rates, and the requirement for a limited operating range. The liquid water removal is studied in order to determine a simple way to deal with the generated liquid water. One way to improve the performance of the cell without the necessity for external humidification would be to use internally generated water to hydrate the membrane and to evaporate the excess water, but this is possible only under certain operating conditions.

Zawodzinski et al. [38] have experimentally investigated the ionic conductivity of the membrane in relation to the water activity, i.e. relative humidity for commercial Nafion® 117 membrane at the temperature of 30°C. They have related the membrane water content with the relative humidity of the reactants by a third degree polynomial expression, which is today commonly used in modeling by various groups of authors. However, the operating temperature of 30°C is quite low, since the PEM fuel cells usually operate at temperatures of 60-80°C, and the membrane thickness is high when compared to currently commercially used membranes. Therefore, the results should be investigated to determine if the expression is valid on higher temperatures.

Hinatsu et al. [39] have investigated the membrane water uptake, i.e. membrane water content for a wide range of operating temperatures, from 25 to 130°C for different

membranes, as well as the Nafion® 117 membrane. The results of the membrane water content in relation to water activity, i.e. relative humidity of the reactants, show similar trend in regions of lower relative humidity when compared to the results of Zawodzinski et al. [38], however, at higher relative humidity of the reactants, the results are quite different. To conclude, if the results of Zawodzinski et al. [38] at temperature of 30°C are quite different from the results of Hinatsu et al. [39] carried out at higher temperatures, then it is not clear why the expression of Zawodzinski et al. [38] is still widely used today. This suggests that the membrane water uptake should be investigated experimentally for thinner membranes as well.

Yang et al. [40] have studied two Nafion® 115 membranes, the first was regular Nafion® 115 membrane, and the other one was Nafion® 115 membrane with 25%wt zirconium phosphate. Both tests were carried out at 80°C. The results of the membrane water content for the two mentioned membranes at different levels of relative humidity show significant difference between the two. The membrane doped with zirconium phosphate has shown higher membrane water content on high relative humidity levels. This work also shows that different additives in the membrane and temperature also influence the membrane water content, therefore the commonly used membrane water content models deserve further scrutiny.

The water management of PEM fuel cells is directly related to two dominant water transport mechanisms through the membrane. Since high membrane water content is of paramount importance for high efficiency performance of the cell, the water transport through the membrane must be controlled. The water transport through the membrane consists of the electro-osmotic drag, i.e. the number of water molecules dragged by a single hydrogen proton from the anode to the cathode side of the cell, and diffusion, i.e. water concentration gradient driven flux. The diffusion is usually in the direction from the cathode to the anode side of the membrane, since the water is generated in the cathode catalyst layer, and in that case it is termed back-diffusion. The occurrence of water driven flux from the anode to the cathode side happens only in rare cases where the anode side hydration is high and the cathode is dry. There is also a pressure driven water flux in the case where the anode and cathode side are at different absolute pressures, but in most practical applications this is not the case. The net water transport through the membrane is then basically a balance between the electro-osmotic drag and back-diffusion flux.

Husar et al. [41] have investigated the water transport through the membrane for the three mechanisms specified above. The pressure driven water flux, termed hydraulic permeation in this work, was at least an order of magnitude lower than the electro-osmotic drag and back-diffusion, therefore it is concluded that it is negligible in practical applications. Each of the water fluxes was investigated separately, and good agreement is found between the back-diffusion flux determined experimentally and the data from the literature being used in this work. The electro-osmotic drag, however, was determined to increase with temperature and current density, contrary to other models in the literature, Fig. 6.

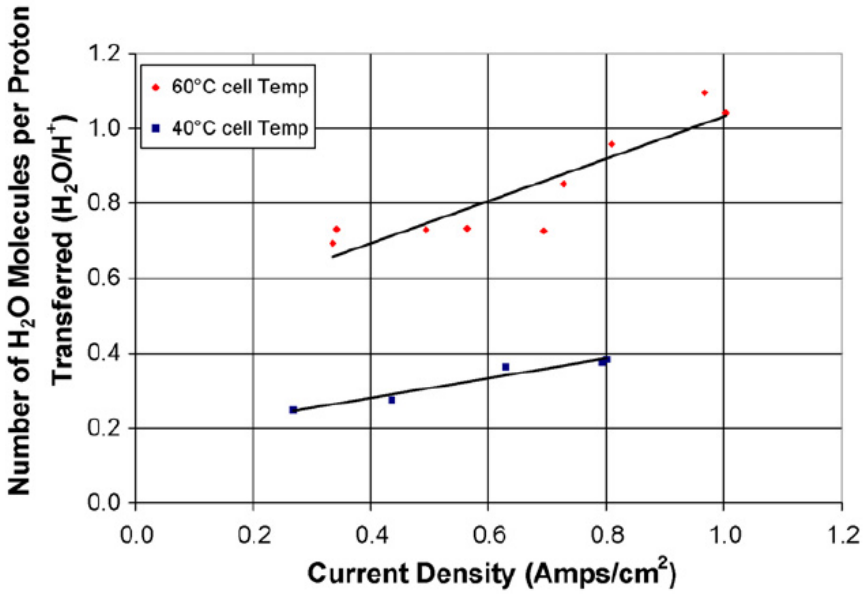

Figure 6. Number of water molecules transferred through the membrane per proton due to electro-osmotic drag at different current densities, adopted from [41].

This work investigated the back-diffusion only on open circuit voltage, at identical operating pressures on the anode and cathode side of the membrane. The open circuit voltage was used to omit the influence of the electro-osmotic drag, however it cannot be seen if the back-diffusion flux changes with the operating current density, therefore a more detailed study should be made.

Jinnouchi et al. [42] have investigated the electro-osmotic drag water flux through Nafion® 112 membrane in correlation to the relative humidity, since this was a common approach and most of the models are based on correlating the relative humidity with the electro-osmotic drag coefficient solely. Their conclusion was that the electro-osmotic drag

is independent on the relative humidity of the reactants, contrary to most of the models in other works, Fig. 7.

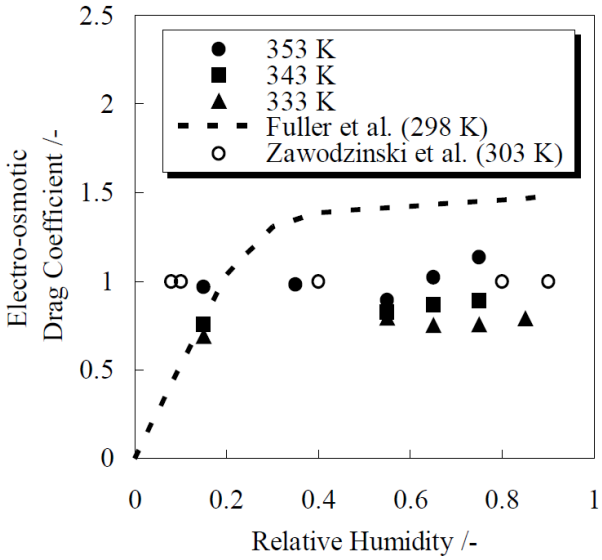

Figure 7. Electro-osmotic drag coefficient of Nafion® for various relative humidity and temperature, adopted from [42].

They have also observed that the electro-osmotic drag coefficient proportionally increases with the increase in temperature, similar to the observations of Husar et al. [41]. The two works [41,42] lead to a conclusion that the electro-osmotic drag models commonly used need to be investigated in more detail experimentally.

Olesen et al. [43] have noted that the commonly used back-diffusion model from Motupally et al. [44], correlating the back-diffusion flux to the membrane water content has a peak value of back-diffusion coefficient for the membrane water content value of 3. The model with the peak back-diffusion value at membrane water content of 3 is also known as Motupally [44] model. The Motupally model is commonly used in various numerical models and shows good agreement with experimental data for higher membrane water content intervals, i.e. higher membrane hydration levels. However, the peak value was not previously explained by other authors. The investigation of the Motupally [44] back-diffusion coefficient model resulted in the conclusion that the peak value at membrane water content value of 3 is simply due to the derivation of the third degree polynomial derived by Zawodzinski et al. [38]. If some other expression is used, for example a higher degree polynomial, or some other function to fit the experimental data point values of Zawodzinski et al. [38], the extreme value at membrane water content value of 3 would not exist. Olesen et al. [43] have derived a new expression for back-diffusion

flux which shows good agreement with experimental data from other authors. This work shows that basic mathematical operations used for determining certain operating parameters can cause confusion, and that the models must be first validated experimentally if some unfamiliar phenomenon is observed in the model. Olesen et al. [43] have also noted the difference between the membrane water content at 30°C and 80°C, as previously explained in investigation of works [41] and [42], as seen in Fig. 8. They have concluded that the membrane water content must be measured at different temperatures and an expression needs to be derived to determine the correlation of the membrane water content to the temperature, and not solely to the relative humidity of the reactants even though the relative humidity of the reactants is already a function of temperature.

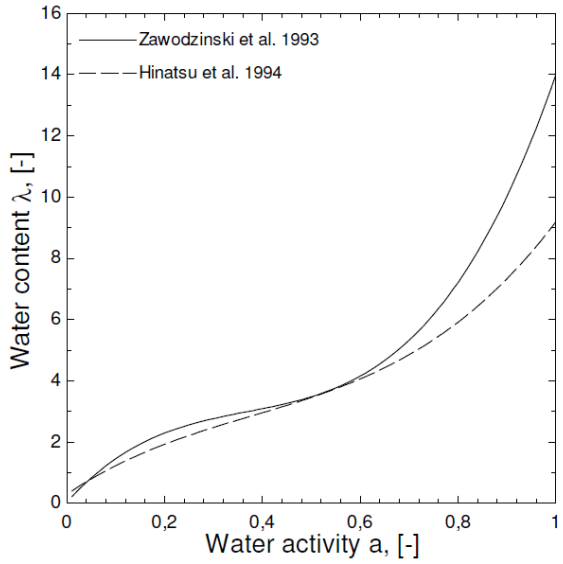

Figure 8. Comparison of membrane water content expressions of Zawodzinski [38] and Hinatsu [41], adopted from [43].

Besides water transport through the membrane, a lot of attention in the literature is recently devoted to the removal of liquid water from the cell. The liquid water is generated in the cell from the electrochemical reaction of the reactants – hydrogen and oxygen, in the cathode catalyst layer. Since the reactants are commonly humidified before the entry to the cell via external humidifiers, the reactants are only able to evaporate small quantities of the generated liquid water. The liquid water is transported through the membrane by the balance of the electro-osmotic drag and back-diffusion, in direction from the anode to the cathode side and vice versa, respectively. The occurrence of liquid water results in pooling of the catalyst layers and the gas diffusion layers from both sides of the membrane. This usually happens at higher current densities, since the amount of generated water is

proportional to the operating current density. The pooling of the pores of gas diffusion layers causes un-even reactant distribution along the membrane active area, i.e. the catalyst layer surface, since the reactants are unable to pass through liquid water. A more pronounced pooling can cause channel flooding, i.e. the occurrence of a liquid water plug flow, which can result in starvation of the cell which must be prevented at all times. For this reason, a couple of important works in the literature are outlined to give a better insight in the water removal strategies and the methods for observing the occurrence of the water flooding inside an operating cell.

Hussaini and Wang [45] have designed an operating PEM fuel cell with the cathode side covered by a transparent Lexan plate, thereby enabling in situ visualization of the liquid water occurrence and transport through the cell. They have distinguished three different liquid water two-phase flow patterns inside the micro flow channels – droplets, film flow and slug flow, as seen in Fig. 9. Although transparent cell can give a qualitative overview of the liquid water transport through the cell, it is not very useful for analytical study since the perception of the liquid water volume fraction is very poor and cannot be precisely determined from a two-dimensional view. The reflective nature of the gas diffusion layers also hinders the potential of determining the volume fraction of the liquid water inside the cell. Therefore transparent cell methods have limited practical applications.

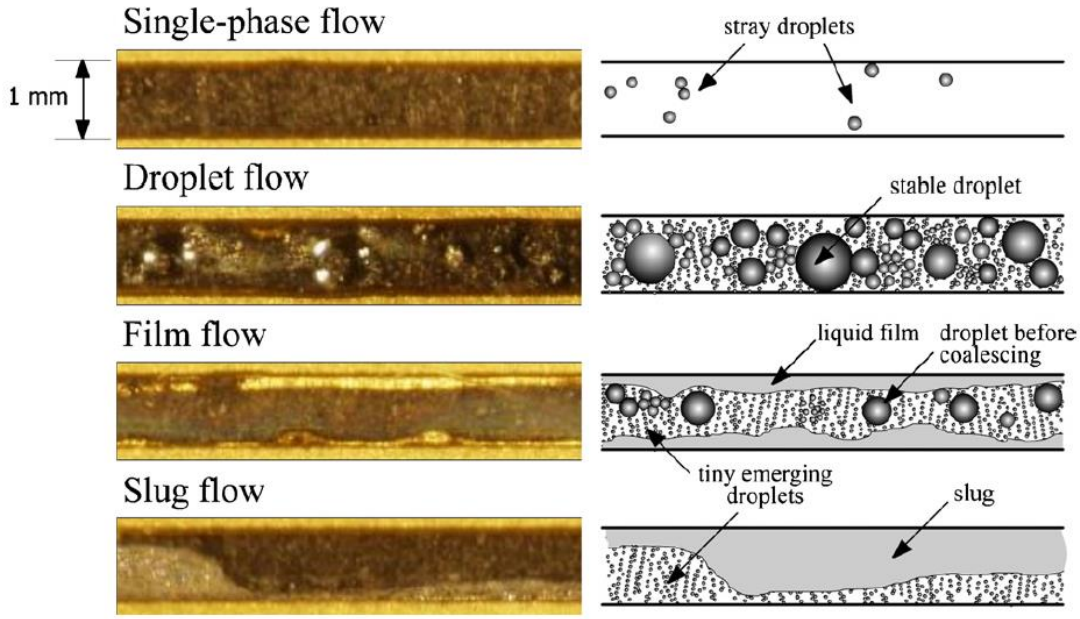

Figure 9. Magnified view of flow patterns in channels and their corresponding line illustrations showing the form and distribution of liquid water, adopted from [45].

Perrin et al. [46] investigated the dynamic water transport for two types of ionomer membranes, Nafion® and sulfonated polyimide by field-cycling nuclear magnetic resonance relaxation. The polyimide membrane has shown higher wettability when compared to the Nafion® membrane. The nuclear magnetic resonance gives valuable information in regard to the liquid water occurrence in the membrane and the reactant channels, as well as the information on the water transport on a nano-scale level through the membrane pores. However, it shows limited practicality for determining the amount of water inside the porous gas diffusion and the catalyst layers, since the gas diffusion layers are made from paramagnetic carbon. Other drawbacks are the limited temporal and in-plane resolution, and the limited size of the magnet-core for housing a complete PEM fuel cell system.

Mosdale et al. [47] have performed a pioneering work in determining the liquid water distribution inside an operating cell via neutron imaging. The neutron imaging is based on a sensitive response of neutrons to hydrogen-containing compounds, such as water, and insensitivity to commonly used PEM fuel cell structural materials. It is currently the only known tool which meets all three requirements for diagnostics of the liquid water distribution inside PEM fuel cell – localized information on liquid water distribution, minimal invasiveness and in situ applicability. Neutron imaging enables in depth visualization of the dynamic liquid water distribution and transport during PEM fuel cell operation and gives insight in the quantitative values of the liquid water volume and droplet size spatial distributions. The main drawbacks of the neutron imaging are its high costs and the requirement for radioactive neutron source.

Turhan et al. [48] have employed the neutron imaging in order to investigate the effect of different reactant channels surface hydrophilic/hydrophobic properties on the liquid water transport inside an operating cell, to determine which configuration is more favorable for PEM fuel cell operation. The hydrophilic configuration consisted of gold coated channel walls, while the hydrophobic configuration consisted of polytetrafluorethylene coated channel walls. It was determined that the hydrophilic configuration is more favorable in terms of more stable water transport, since the liquid water is transported in forms of a thin water film on the channel walls, thereby not obstructing the flow of the reactants through the gas diffusion layers and consequently the catalyst, as seen in Fig. 10.

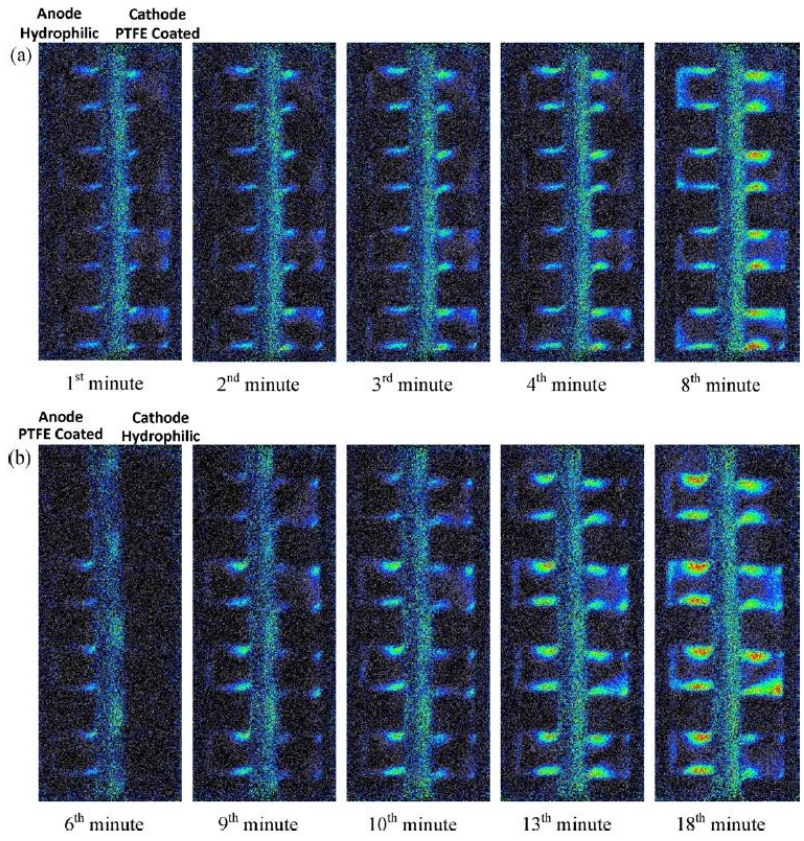

Figure 10. Neutron images of water build-up in gas diffusion layers and water discharge into channels at 0.2 Acm^{-2} operation for (a) anode channel hydrophilic (gold coated)/cathode channel hydrophobic (polytetrafluoethylene coated) and (b) anode channel hydrophobic (polytetrafluorethylene coated)/cathode channel hydrophilic (gold coated), adopted from [48].

However, the water removal was slower with hydrophilic walls since the cross section of the liquid water in respect to the reactants was lower, and the required drag force for pushing the droplets was higher. Also, the accumulation of the liquid water below the land – gas diffusion layer interfaces was higher when compared to the hydrophobic reactant channel configuration. The hydrophobic channel walls resulted in faster water removal from the channels in the form of water droplets, unlike the water film for the hydrophilic case, and higher water removal rates from the land-gas diffusion layer interfaces. However, the hydrophobic walls resulted in water droplet removal across the gas diffusion layer – channel interface, thereby reducing the active area for the reactant passage through the gas diffusion layer. From this work it can be concluded that the optimal combination would be to design the flow field with hydrophilic channel walls and hydrophobic land – gas diffusion layer interfaces. Also, since the geometry of the setup in work [48] of the channels was simple parallel channel design, it would be advisable to also

conduct the experiments on more complex flow field geometry, i.e. interdigitated or serpentine type flow fields.

3.2.1 Conclusions

The general conclusion of the water management investigation is that the most fundamental physical property of the membrane, the membrane water content, on which every analytical model is based, deserves further scrutiny. The same conclusion can be drawn from investigation of different experimental results for very similar configurations and operating conditions of PEM fuel cells. The investigation of liquid water transport inside an operating cell is complex and requires costly equipment, such as neutron imaging. The best option would be to develop a new experimental setup which will enable measurement of the water transport through the membrane and development of the membrane water content expression for different temperatures to avoid using potentially erroneous analytical models. Since the investigation of the occurence of liquid water inside an operating cell results in potentially catastrophic failure of the cell, it would be best to minimize the amount of liquid water inside the cell. For this reason, it would be advisable to investigate the concept of a variable temperature flow field mentioned in the previous chapter, to enable evaporation of the generated liquid water and to use the generated water vapor to saturate the reactant gases close to 100%. The most suitable tool for investigation of such concept would be a computational fluid dynamics model, which will need to be thoroughly calibrated with some experimental test case.

3.3 Computational fluid dynamics modeling of PEM fuel cells

Computational fluid dynamics (CFD) modeling becomes a common practice in recent years due to development of high performance personal computers, since the application of CFD modeling was only possible on super computers beforehand. CFD modeling enables detailed insight in distributions of local parameters inside an operating cell. However, the CFD model must be validated with experimental data due to very high number of input data required for precise and credible simulations. Even though most of the researchers use commercial softwares, it is still a challenge to develop a robust PEM fuel cell model due to the requirement for high number of experimental input parameters and the multi-disciplinary knowledge required for explanation of different phenomena inside an operating cell.

Gurau et al. [49] have made the first CFD model of a PEM fuel cell. The model was two-dimensional but it incorporated most of the physical processes inside an operating cell. The work of Gurau et al. [49] resulted in of PEM fuel cell add-ons of commercial CFD softwares. However, the two-dimensional model is a dramatic simplification of PEM fuel cell, since it does not consider the non-uniform distribution of current density, reactant concentration, relative humidity, temperature, etc. The conclusion is that the CFD model of PEM fuel cell must be three-dimensional, even for the simplest flow field geometries. Interesting detail in this work is that the agreement of the simulation results and the experimental data for polarization curve is very good, Fig. 11, even though the model is dramatically simplified, leading to a conclusion that in order to have a validated model, one should also compare the local parameters with the experimental data.

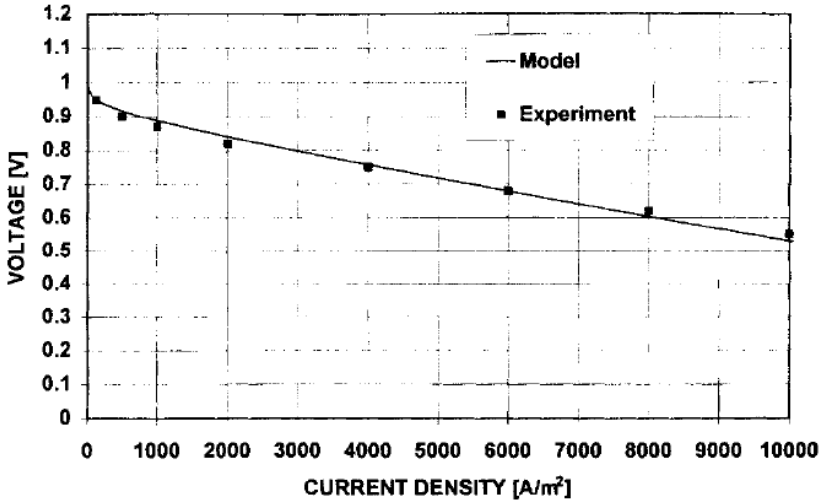

Figure 11. Model and experimental polarization curves, adopted from [49].

Shimpalee et al. [50] have developed first full-scale CFD model of a commercial size PEM fuel cell. The cell had active area of 480 cm^2, the flow field is shown in Fig. 12. The results of the simulations carried out in this work show that the operating parameters inside PEM fuel cell, such as temperature, current density and membrane water content are non-uniformly distributed. The non-uniformity of the parameters is strongly influenced by relative humidity of the reactants upon the entry to the cell. Unfortunately, the calibration and experimental validation has not been done in this work, but it was demonstrated that CFD gives valuable insight in multiphysical phenomena inside an operating cell.

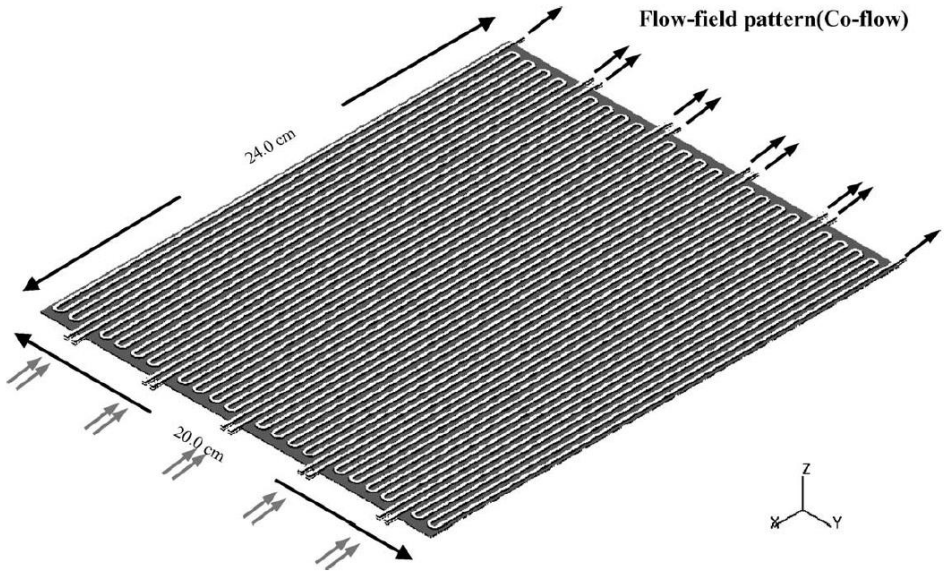

Figure 12. Flow field of a commercial 480cm^2 PEM fuel cell, adopted from [50]

Berning and Djilali [51] have carried out a parametric investigation on their previously developed CFD model, the results are shown in Fig. 13. The simulation results have been compared to other experimental data in the literature with good agreement. The conclusion of this work is that in order to simulate the limiting current density occurance, it is advisable to manipulate the porosity of the gas diffusion layer, i.e. the reduction in the porosity due to accumulation of liquid water inside the gas diffusion layer pores at higher current densities. However, only the global simulation parameters have been compared to the experimental data, such as power curves and polarization curves. The localized data was not compared, therefore the capability of the model in predicting the local parameter distributions is unclear.

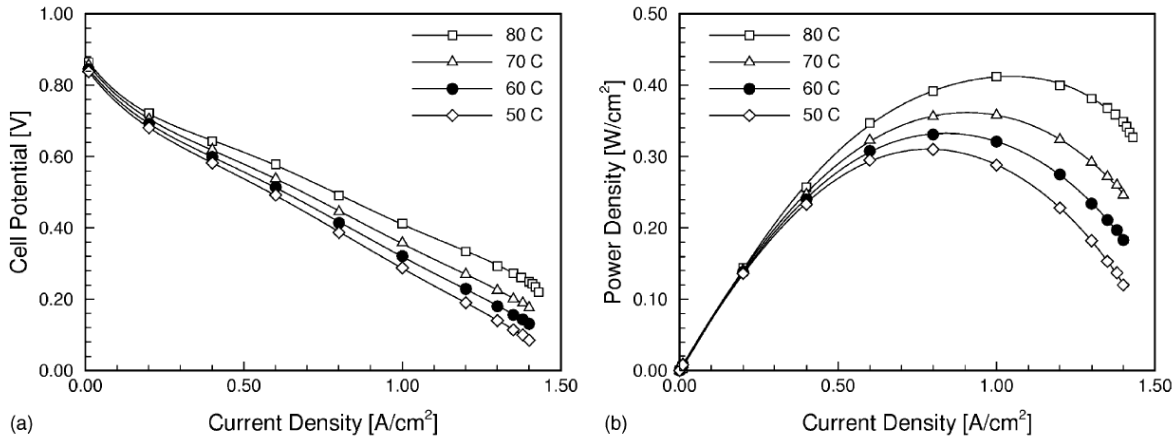

Figure 13. Predicted polarizaton curves (a) and power density curves (b) for different cell temperature, adopted from [51].

Lum and McGuirk [52] have developed a CFD model similar to the one of Shimpalee et al. [50]. They have validated the model on a global and local scale. The global validation was carried out by comparing the polarization and power curves with the experimental data. The local validation is achieved by comparing the current density distribution with the experimental data from a segmented fuel cell, as seen in Fig. 14. The model data shows good agreement with the experimental data for global and local comparison. However, the relative humidity profiles along the channel length have not been compared with the experimental data, therefore it is not clear if the model is credible in terms of water transport through the membrane.

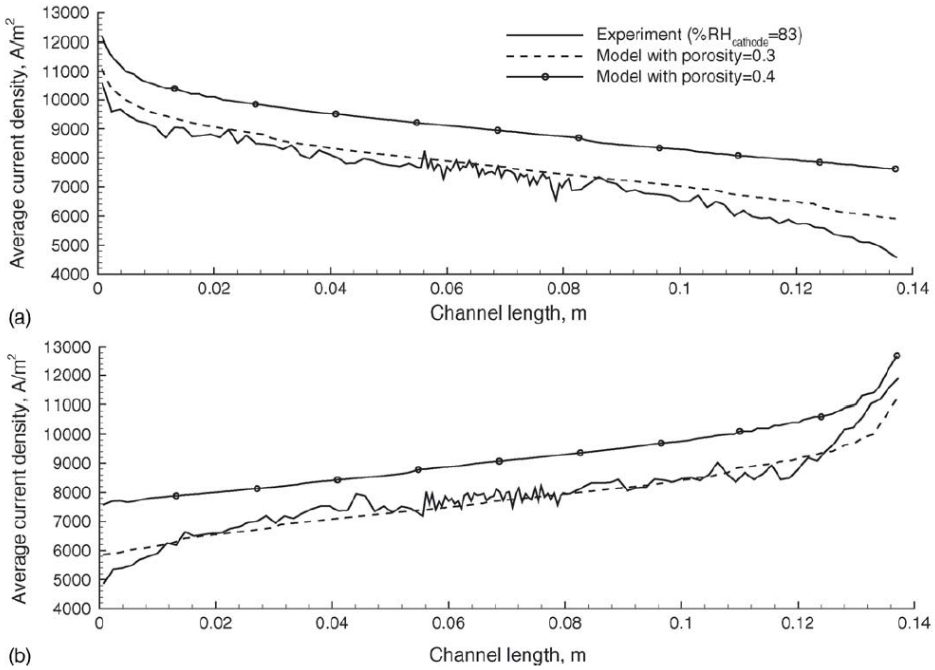

Figure 14. Comparison of local current density distribution along the cathode side of the cell of models with different porosity with experimental data, for (a) co-flow and (b) counter-flow, adopted from [52].

Ozden et al. [37] have developed a CFD model based on geometric and operating parameters from the work of Tolj et al. [8]. The CFD model was used to investigate the capability of simulating the PEM fuel cell operation with prescribed variable temperature flow field which was introduced in terms of spatially variable heat removal rates. The comparisonof the modeling and experimental results was carried out for operating current density of 500 mAcm^{-2} with good agreement on a global scale, i.e. polarization curve, for isothermal and variable temperature flow field cases. However, the comparison of the

relative humidity profiles along the cathode channel length with the experimental data was different, i.e. the relative humidity profiles apeared similar to the experimental results but were shifted to higher values, and the explanation for this behaviour was not clear. This leads to a conclusion that the CFD models need to be verified with relative humidity profiles along the channel length, as well as the current density distribution along the cell to have a credible CFD PEM fuel cell model.

The CFD modeling of PEM fuel cell stacks has only been done by a couple of researchers, due to high computational requirements and convergence issues involved in such simulations.

Liu et al. [53] have published the first work dealing with CFD simulations of a PEM fuel cell stack. However, the whole stack was dramatically simplified and modeled as a porous zone. The reactant depletion and water generation was simulated by sink and source terms, as well as the accompanying heat sources. The results of the simulations are not realistic due to the fact that the lands and channels represent a single porous zone, therefore the relative humidity distribution along the entire flow field is not correct. Since the membrane water content is a function of the relative humidity of the reactants, it is also not correct, as well as the current density distribution along the entire flow field. It is interesting to see that the polarization curve prediction of the CFD model is very good when compared to the experimental polarization curve. This leads to a conclusion that in order to develop a credible model, it is a must to have local parameter validation. This work shows an interesting phenomenon of slight rise in overall temperature in the cathode direction of the stack height, Fig. 15.

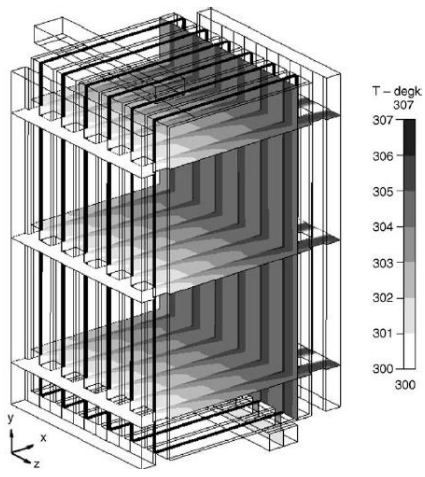

Figure 15. Temperature distribution of the fuel cell stack in *yz* and *zx* directions, adopted from [53].

Shimpalee et al. [54] have carried out CFD simulations for a six cell portable, air-cooled PEM fuel cell stack. The results of the simulations have been compared with experimental data on a global scale, i.e. polarization curves, for each of the cells in the stack. The simulation results have shown good agreement with experimental results. It is noted that the top and bottom cell of the stack shows the highest performance, while the cells in the center show lower performance. The stoichiometry of the reactants was quite high, in order of 4-5. Different performance of the cells in the stack is not elaborated in detail. The fact that the top and bottom cell show the highest performance can be clearly attributed to higher heat removal rates due to the presence of thick aluminium blocks on the experimental installation, however it is unclear how this was achieved numerically since the requirement for such numerical results requires defining heat sinks at the top and bottom of the stack, or prescribind fixed temperature boundary conditions would be non-physical for this case, and the boundary conditions of such types have not been mentioned. The clear indication of this work is that the operating parameters show non-uniformity along the stack height as well as along the flow field of each cell, therefore it is required to simulate operation of more than one single cell to get insight in the performance of the whole stack.

Macedo-Valencia et al. [55] have carried out CFD simulations for a five cell PEM fuel cell stack. The agreement with the experimental results is not as good as in the work of Shimpalee et al. [54]. The temperature gradient is visible along the stack height, with slightly higher temperature in the cathode direction, Fig. 16, but the end plates seem to be of similar temperatures, probably due to prescribed fixed temperature boundary conditions along the current collector surfaces, instead of adiabatic walls or a fixed heat flux, since the fixed temperature boundary condition in this case would be non-physical. The boundary conditions on the current collectors are not specified in this work, and it is simply noted that this behaviour is less eminent for higher electric potentials, i.e. lower electrical currents.

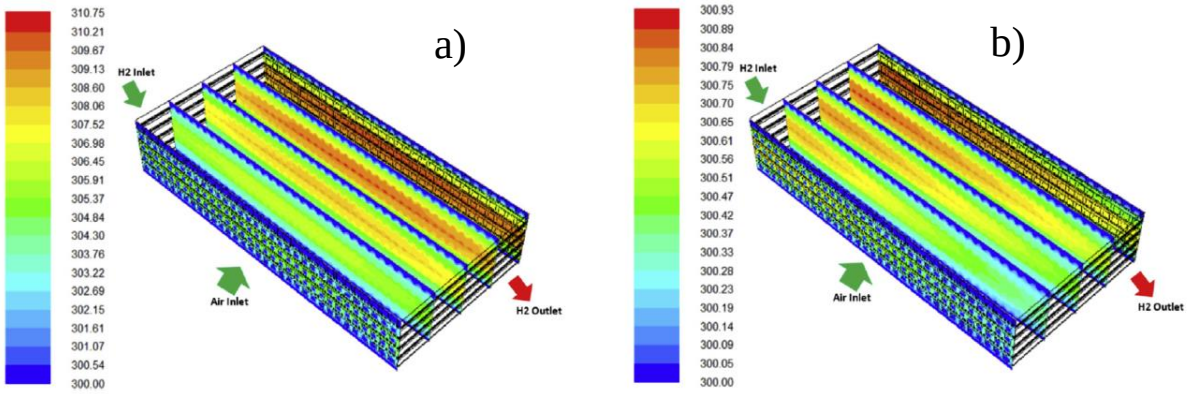

Figure 16. Temperature distributions (K) along the PEM fuel cell stack width at a) 0.6 V and b) 0.8 V, adopted from [55].

3.3.1 Conclusions

Computational fluid dynamics are a very useful tool for insight in the parameter distributions inside the operating PEM fuel cell. The literature survey shows that the commercially used softwares have good capability for predicting PEM fuel cell performance, however the main requirement for development of a credible CFD model is to have experimental results which can be used to validation of the model. However, the global parameters commonly used in PEM fuel cell society, such as the polarization curves and power curves, are not sufficient for validation of the CFD model. To validate the model, one must also consider the local parameter distributions, such as current density and relative humidity along the entire flow field. The conclusion is that in order to develop a robust and credible CFD model, a robust experimental installation is required which will enable the measurement of operating parameters locally, namely current density, relative humidity and temperature. This leads to the requirement for development of a segmented PEM fuel cell. It is interesting to see that none of the CFD modeling works in the literature deal with analysis of PEM fuel cell operation under prescribed variable temperature flow field by means of mass flow rate control of the coolant.

3.4 Segmented PEM fuel cell

In order to have insight in the local distribution of operating parameters, such as current density, relative humidity and temperature, it is required to design a segmented PEM fuel cell. Segmented cell represents a single PEM fuel cell which is assembled of a certain number of smaller parts, i.e. segments. Each of the segments is connected in parallel electrically and in series in respect to the flow of the reactants. The total operating current is sum of electrical currents on each segment, while the reactants enter each

segment with the species concentration, relative humidity and temperature determined by the inlet parameters of the reactants as well as the electrochemical and thermodynamical aspects which are a consequence of the reactant passage through the previous segment – the one closer to the inlet in respect to the reactant, be it anode or cathode and co-flow or counter-flow configuration. The bipolar plates are composed of a number of segments which are insulated electrically and thermally from the neighboring segments and connected to a data acquisition instrument. The segments are then connected electrically together to a common current collector in order to enable measurement of electrical current, and in some cases temperature, of each segment. Additionally, relative humidity and temperature sensors can be placed between the neighboring segments to give insight in the temperature and relative humidity of the reactants from both sides of the membrane, the anode and the cathode. If such segmented fuel cell is assembled, it can be used for thorough validation of a developed CFD model for different sets of input parameters. Once the CFD model is developed and validated with high credibility, i.e. good agreement of global and local parameters, it can be used for studying the effect of using different flow field configurations, gas diffusion layers, catalyst layers and membranes and operating parameters on PEM fuel cell performance. Since there area many works dealing with segmented PEM fuel cells, only a few of them will be addressed in this chapter, since the goal of the research is to design a segmented fuel cell which will enable measurement of relative humidity profiles, temperature profiles and current density along the entire flow field. Also, since variable temperature flow field is of interest in this work, a method for establishing a variable temperature flow field in such setup will be discussed.

Tolj et al. [8] have developed a segmented PEM fuel cell with capability of measuring the relative humidity distributions along the cathode side of the cell. The segmented cell consisted of five single cells connected electrically in parallel, and in series in respect to the reactant flow, Fig. 17.

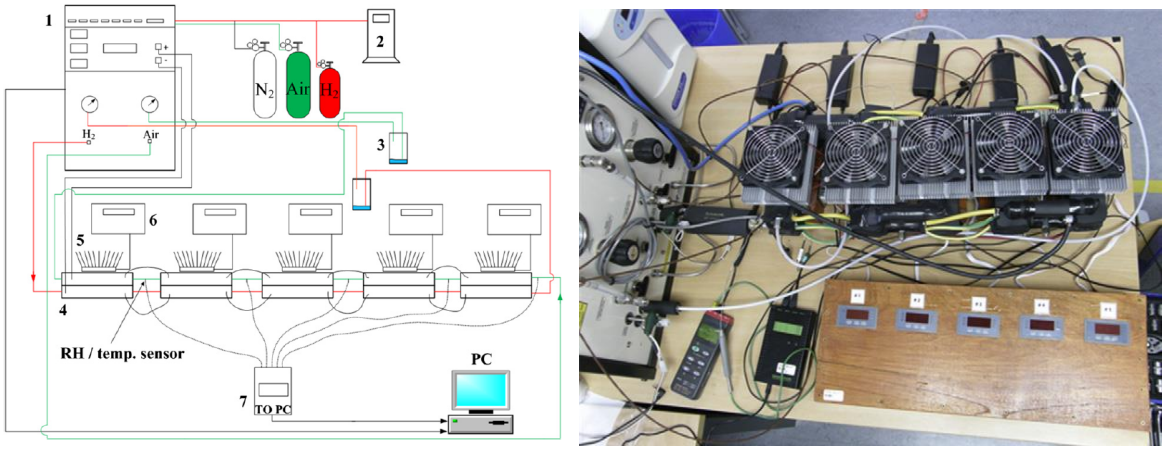

Figure 17. Left - Schematic setup of experimental segmented fuel cell: (1) fuel cell test station; (2) hydrogen generator; (3) water trap; (4) fuel cell segment; (5) Peltier thermoelement; (6) temperature controller; (7) data acquisition for relative humidity and temperature sensors. Right – Experimental setup, adopted from [8].

The reactants enter the first segment with prescribed conditions: stoichiometry, absolute pressure, temperature and relative humidity. After passing through the segment, a part of the reactants will be depleted, and a certain amount of water will be generated. This will result in different relative humidity and temperature of the reactants, as well as different concentration of the oxydant and fuel on the outlet from the segment. Reactants with such composition enter the next segment, etc. The interesting details about this work is the study of influence of a variable temperature flow field on PEM fuel cell performance. The temperature of each segment was regulated by Peltier thermoelements placed on the cathode side of the cell. The prescribed temperature profile was adjusted to resemble water vapor saturation temperature from Mollier's *h-x* chart for the calculated amount of generated water. The experimental results have shown that it is possible to achieve high performance of the cell without the necessity for external humidification, with dry hydrogen supply on the anode and ambient air supply on the cathode. However, the relative humidity along the anode side was not measured, and the temperature on the anode side was not regulated by Peltier thermoelements, therefore the water transport through the membrane could not be investigated. The experimental setup with five separate cells also resulted in condensation of the water vapor between each of the segments since the insulation was not sufficient to avoid this problem. The condensation of water vapor created problems during measurements since the relative humidity and temperature sensors had to be dried before and after each set of measurements.

Yin et al. [26] have developed a segmented PEM fuel cell recently with capability of measuring current density, relative humidity and temperature along the cell with parallel channels, Fig. 18. The copper current collectors are gold plated and of a printed circuit board type, and the temperature profile is regulated by the mass flow rate control of the coolant fluid.

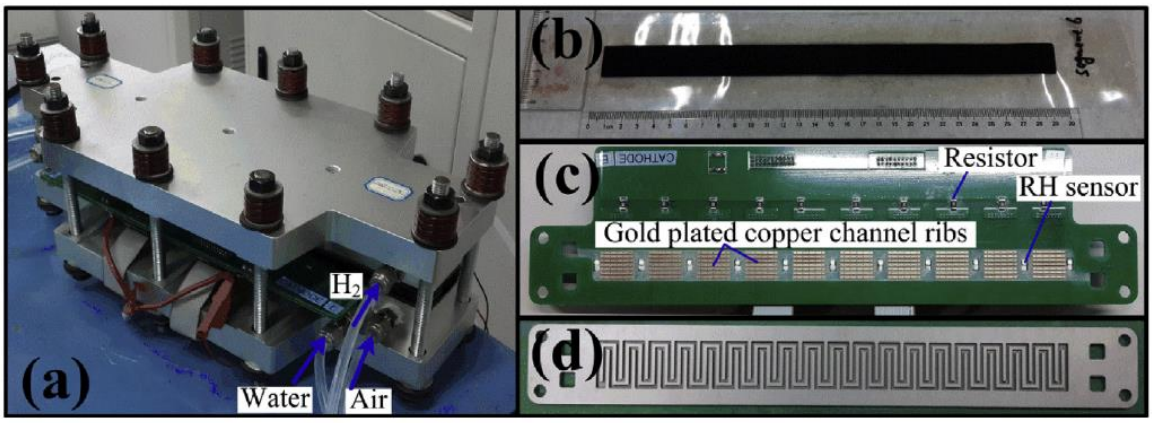

Figure 18. Segmented fuel cell with its main components: (a) segmented fuel cell assembly; (b) MEA; (c) reactant distribution plate based on multi-layered printed-circuit board plate with current and relative humidity sensors; (d) coolant water graphite plate with serpentine flow channels, adopted from [26].

The flow configuration in their study is co-flow between the reactants and the coolant. This design would be very suitable for developing a robust and credible CFD model, since it also gives insight in the membrane water transport, therefore the effort of this work is to develop similar concept. However, to maximize the performance of the cell in the work of Yin et al. [26] it would be advisable to set the reactants in counter-flow, and the coolant in co-flow with the cathode air, to use parallel channels for the coolant instead of serpentines, and to prescribe the temperature profile using Mollier's *h-x* chart, as done in the work of Tolj et al. [8].

3.4.1 Conclusions

Segmented PEM fuel cell is the most suitable experimental setup for developing a robust CFD model with capability of predicting PEM fuel cell performance for various configurations of operating and structural parameters. The segmented PEM fuel cell will need to have capability of measuring the current density, relative humidity and temperature distribution along the entire flow field. The segmented cell can then be used to develop a CFD model for variable temperature flow field to maximize the performance of the cell fed

with dry hydrogen and ambient air, where the temperature profile can be prescribed for different operating current densities. The desired temperature profile can be extracted from Mollier's *h*-*x* chart for the calculated amount of generated water.

4 CONCLUSIONS

The efficiency of PEM fuel cell is closely related to the membrane water content, and the membrane water content is dependent upon the relative humidity of the reactants – hydrogen and air. Since the relative humidity depends on the amount of water in the reactant stream at a certain temperature, it is easy to see that the water and heat management are of paramount importance for PEM fuel cell operation. Therefore this work focuses primarily on the current state-of-the art regarding the two.

The heat management chapter leads to a conclusion that in order to design a system for sufficient removal for high performance PEM fuel cell stack, it is best to use the coolant fluid. Common approach of keeping the temperature uniform along the entire flow field is brought into question by certain authors, since it results in non-uniform performance of the cell. Therefore it is suggested to study the influence of a non-uniform temperature flow field which will result in close to 100% relative humidity along the entire flow field, by using internally generated water for internal humidification of the reactants and heat for establishment of such temperature profile. However, the exact method for establishing such operation is not mentioned.

The water management chapter deals with works in the literature commonly cited by vast number of other researchers, but it also brings into the question the discrepancies between different groups of authors regarding the measurements of the two dominant membrane water transport mechanisms – electro-osmotic drag and back-diffusion. It can be seen that the membrane water content equation broadly used today shows relatively high discrepancies with more recent works dealing with experimental measurements of membrane water content at higher temperatures. Since the original equation was derived for operating temperature of 30°C, and the expression for operating temperature of 80°C is quite different, the original expression for 30°C deserves further investigation, at higher temperatures and for different membrane thicknesses. Other works in this chapter deal with the problematic water removal and its effect on the PEM fuel cell system, and the overall conclusion is that it would be best to minimize the amount of generated water by evaporating the generated liquid water in the stream of reactants. Such operation, combined with proper heat management, would lead to a PEM fuel cell system without the requirement for external humidification, nor the hydrogen recirculation pump. Such system would be novel, since the method for achieving such operation on a PEM fuel cell stack

level has not yet been achieved, and the complexity and costs of such system would be significantly reduced.

The computational fluid dynamics modeling of PEM fuel cells chapter gives a brief introduction in the modeling of PEM fuel cells, from obsolete two-dimensional modeling to highly complex modeling of PEM fuel cell stacks. The results from researchers show that in order to develop a high credibility CFD model, one must achieve good agreement of global parameters, such as the polarization curve or power curve, and also of local parameters, the most important one being the current density distribution and the relative humidity distribution, with the experimental data. A couple of works in this chapter show good agreement with experimental polarization curves, but the results of local parameter distributions show high discrepancies with the experimental results. The most prominent tool for development of a robust and credible CFD model would be to design a segmented PEM fuel cell, with the possibility to prescribe a custom temperature flow field, with measurements of relative humidity, temperature, and current density on each segment.

The segmented PEM fuel cell chapter gives examples of two interesting candidates for developing the experimental segmented fuel cell for future studies. The more recent work [26] dealing with segmented PEM fuel cell shows that it is possible to establish a temperature gradient along the cell by using internally generated heat to establish the temperature profile of the coolant, therefore it is not required to establish the temperature profile by using external thermoelements. Once developed, the segmented PEM fuel cell experimental setup will enable development of a highly credible CFD model, which will be used to study the performance of PEM fuel cell under various operating parameters, variable temperature flow field, and various structural configurations on single cell and stack level.

Future studies will deal with development of advanced segmented fuel cell setup with capability of measuring the relative humidity, temperature and current density profiles along the channel length. The CFD model will be developed and calibrated to enable investigation of the influence of non-uniform temperature flow field on PEM fuel cell performance, and used to determine if it would be feasible to develop a PEM fuel cell stack with coolant loop which will be used to prescribe the desired temperature profile and enable high efficiency PEM fuel cell stack operation without the necessity for external humidification for the first time.

5 ACKNOWLEDGEMENTS

The research leading to these results has received funding from the Croatian Science Foundation project IP-11-2013-8700 “Water and Heat Management and Durability of PEM Fuel Cells“. Ž. Penga also acknowledges support he has received from EU FP7 Programme through Fuel Cells and Hydrogen Joint Undertaking under grant agreement n° 325275 (Project SAPPHIRE).

6 LIST OF SYMBOLS[1]

General symbols

a – water activity

CFD – Computational fluid dynamics

c_r – condensation rate constant, s^{-1}

D_i – gas phase species diffusivity, m^2s^{-1}

D_l – membrane water diffusivity

D_i^0 – species mass diffusivity, m^2s^{-1}

D_{eff}^{ij} – effective gas species diffusivity, m^2s^{-1}

e – electron

F – Faraday constant, $Ckmol^{-1}$

g – gravitational acceleration, ms^{-2}

H – hydrogen

h – enthalpy, J

h_L – source term for enthalpy of water phase change, Wm^{-3}

h_{react} – electrochemical heat source, Wm^{-3}

I – electrical current, A

I_{leak} –leakage current, A

J_w^{diff} – back diffusion flux, $kgm^{-3}s^{-1}$

j^{ref} – exchange current density per active surface area, Am^{-2}

K – absolute permeability

k^{eff} – thermal conductivity, $Wm^{-1}K^{-1}$

M_m – equivalent weight of the dry membrane, $gmol^{-1}$

M_i – molar mass of species, $gmol^{-1}$

[1] Symbols adopted from Fluent Fuel Cell Module Manual®

n_d – electro-osmotic drag coefficient

O – oxygen

p – pressure/local pressure, Nm^{-2}

PEM – proton exchange membrane

p_c – capillary pressure, Nm^{-2}

p_{sat} – water vapor saturation pressure, Nm^{-2}

p_{wv} – partial pressure of water vapor, Nm^{-2}

$\dot{Q}$ – heat flux, W

R – gas constant, $K^{-1}mol^{-1}$

$R_{an/cat}$ – overpotential anode, cathode, V; exchange current density anode/cathode, Am^{-3}

$R_{sol/mem}$ – volumetric transfer current of solid phase/membrane, Am^{-3}

R_{ohm} – ohmic resistance, Ω

r_w – condensation rate, $kgm^{-3}s^{-1}$

r_s – pore blockage exponent

s – volume fraction of liquid water

S_h - source term for heat, Wm^{-3}

S_i – species source/sink term, $kgm^{-3}s^{-1}$

S_{mass} – source term for continuity equation, $kgm^{-3}s^{-1}$

S_{mom} – source term for momentum equation, $kgm^{-3}s^{-1}$

S_T – source term for energy equation, Wm^{-3}

T – temperature, K

V – volume, m^3; electric potential, V

Vol – volume, m^3

$\vec{V}$ – velocity vector, ms^{-1}

$\vec{v}$ – velocity vector, ms^{-1}

x – water vapor mass fraction

X_i – species mass fraction

[ ] – local species concentration, $kmolm^{-3}$

Greek symbols

α – transfer coefficient

β – electrolyte electrical conductivity generalization constant

γ – concentration dependency coefficient; function exponent

ε - porosity

ζ – specific active surface area, m^2

η – local overpotential, V

$\eta_{an,cat}$ – transition current anode, cathode, Am^{-3}

θ – contact angle, °

λ – membrane water content

μ – dynamic viscosity, $kgm^{-1}s^{-1}$

ρ – density, $kg\ m^{-3}$

ρ_m – dry membrane density, kgm^{-3}

σ – electrical conductivity, $\Omega^{-1}\ s^{-1}$; surface tension, Nm^{-1}

ϕ – electric potential, V

ω – absolute humidity, $kg_{H_2O}kg_{air}^{-1}$; electrolyte electrical conductivity generalization constant

Mathematical symbols

∂ – partial derivative

∇ – nabla operator

General indexes

an - anode

cat – cathode

i - specie

l – liquid water

p - pressure

ref – reference value

t - temperature

0 – reference value

$(+)$ – positive charge

$(-)$ – negative charge

7 REFERENCES

[1] Barbir F. PEM fuel cells, 2nd edition: theory and practice. Academic Press 2012.

[2] EG&G Technical Services, Inc.. Fuel cell handbook. U.S. Department of Energy; 2004.

[3] Zheng CH, Oh CE, Park YI, Cha SW. Fuel economy evaluation of fuel cell hybrid vehicles based on equivalent fuel consumption. Int J Hydrogen Energy 2012;37:1790-6.

[4] Hwang J, Chen Y, Kuo J. The study on the power management system in a fuel cell hybrid vehicle. Int J Hydrogen Energy 2012;37:4476-89.

[5] Simons A, Bauer C. A life-cycle perspective on automotive fuel cells. Appl Energy 2015;157:884-96.

[6] Larminie J. Fuel cell systems explained. West Sussex: Wiley; 2002.

[7] Konno N., Mizuno S., Nakaji H., Ishikawa Y. Development of Compact and High-Performance Fuel Cell Stack. SAE Int. J. Alt. Power 2015;4(1):123-129.

[8] Tolj I, Bezmalinovic D, Barbir F. Maintaining desired level of relative humidity throughout a fuel cell with spatially variable heat removal rates. J Hydrogen Energy 2011;36:13105-13.

[9] Kulikovsky AA, Divisek J, Kornyshev AA. Modeling the cathode compartment of polymer electrolyte fuel cells: Dead and active reaction zones. J Electrochem Soc 1999;146(11):3981-91.

[10] Mazumder S, Cole JV. Rigorous 3-D mathematical modeling of PEM fuel cells II. Model predictions with liquid water transport. J Electrochem Soc 1999;150(11):A1510-17.

[11] Sukkee U, Wang CY, Chen KS. Computational fluid dynamics modeling of proton exchange membrane fuel cells. J Electrochem Soc 1991;147(12):4485-93.

[12] ANSYS, Inc. ANSYS Fluent 12.0 Fuel Cells Module Manual. ANSYS, Inc. 2009.

[13] Nam JH, Karviany M. Effective diffusivity and water-saturation distribution in single- and two-layer PEMFC diffusion medium. I Journal Heat Mass Transfer 2003;46(24):4595-11.

[14] Nguyen TV. Modeling two-phase flow in the porous electrodes of proton exchange membrane fuel cells using the interdigitated flow fields. Tutorials in electrochemical engineering mathematical modeling 1999;99(14):222-41.

[15] Springer TE, Zawodzinski TA, Gottesfeld S. Polymer electrolyte fuel cell model. J Electrochem Soc 1991;138(8):2334-41.

[16] Brandon ME. One-dimensional, transient model of heat, mass, and charge transfer in proton exchange membranes 2001. M.S. Thesis.

[17] Yousfi-Steiner N, Mocoteguy Ph, Candusso D, Hissel D, Hernandez A, Aslaindes A. A review on PEM degradation associated with water management: Impacts, influent factors and characterization. J Power Sources 2008;183:260-74.

[18] Zawodzinski TA, Derouin C, Radzinski S, Sherman RJ, Smith VT, Springer TE, et al. Water uptake by and transport through Nafion 117 membranes. J Electrochem Soc 1993;140:1041-7.

[19] Zhang J, Tang Y, Song C, Cheng X, Zhang J, Wang H. PEM fuel cells operated at 0% relative humidity in the temperature range of 23–120°C. Electrochimica Acta 2007;52:5095-101.

[20] Guvelioglu GH, Stenger HG. Flow rate and humidification effects on a PEM fuel cell performance and operation. J Power Sources 2007;163:882-91.

[21] Song C, Chua JC, Tang Y, Zhang J, Zhang J, Li J et al. Voltage jump during polarization of a PEM fuel cell operated at low relative humidities. J Hydrogen Energy 2008;33:2802-07.

[22] Saleh MM, Okajima T, Hayase M, Kitamura F, Ohsaka T. Exploring the effects of symmetrical and asymmetrical relative humidity on the performance of H2/air PEM fuel cell at different temperatures. J Power Sources 2007;164:503-09.

[23] Jeon DH, Kim KN, Baek SM, Nam JH. The effect of relative humidity of the cathode on the performance and the uniformity of PEM fuel cells, J Hydrogen Energy 2011;36:12499-511.

[24] Bi W, Sun Q, Deng Y, Fuller TF. The effect of humidity and oxygen partial pressure on degradation of Pt/C catalyst in PEM fuel cell. Electrochimica Acta 2009;54:1826-33.

[25] Huang X, Solasi R, Zou Y, Feshler M, Reifsnider K, Condit D et al. Mechanical endurance of polymer electrolyte membrane and PEM fuel cell durability. J Polymer Science 2006;16:2346–57.

[26] Yin C, Gao J, Wen X, Xie G, Yang C, Fang H, Tang H. In situ investigation of proton exchange membrane fuel cell performance with novel segmented cell design and a two-phase flow model. Energy 2016;113:1071-89.

[27] Weng FB, Jou BS, Li CW, Su Ay, Chan SH. The effect of low humidity on the uniformity and stability of segmented PEM fuel cells. J Power Sources 2008;181:251–8.

[28] Chen YS, Peng H. A segmented model for studying water transport in a PEMFC. J Power Sources 2008;185:1179-92.

[29] Weng FB, Hsu CY, Li CW. Experimental investigation of PEM fuel cell aging under current cycling using segmented fuel cell. J Hydrogen Energy 2010;35:3664-75.

[30] Abdullah AM, Okajima T, Mohammad AM, Kitamura F, Ohsaka T. Temperature gradients measurements within a segmented H_2/air PEM fuel cell. J Power Sources 2007;172:209-14.

[31] Berg P, Promislow K, Stumper J. Discharge of a segmented polymer electrolyte membrane fuel cell. J Fuel Cell Science and Technology 2005;2:111-21.

[32] Zhang G, Kandlikar SG. A critical review of cooling techniques in proton exchange membrane fuel cell stacks. J Hydrogen Energy 2012;37:2412-29.

[33] Chen FG, Gao Z, Loutfy RO, Hecht M. Analysis of optimal heat transfer in a PEM fuel cell cooling plate. Fuel Cells 2003;3(4):181-8.

[34] Mench MM. Fuel cell engines. Hoboken: John Wiley & Sons; 2008.

[35] Wilkinson DP, Voss HH, Fletcher NJ, Johnson MC, Pow EG. Electrochemical fuel cell stack with concurrent flow of coolant and oxidant streams and countercurrent flow of fuel and oxidant streams. US Patent 5773160; 1998.

[36] Kang S, Min K, Mueller F, Brouwer J. Configuration effects of air, fuel, and coolant inlets on the performance of a proton exchange membrane fuel cell for automotive applications. J Hydrogen Energy 2009;34:6749-64.

[37] Ozden E, Tolj I, Barbir F. Designing heat exchanger with spatially variable surface area for passive cooling of PEM fuel cell. Applied Therm Eng 2013;51(1-2):1339-44.

[38] Zawodzinski TA, Derouin C, Radzinski S, Sherman RJ, Smith VT, Springer TE, et al. Water uptake by and transport through Nafion 117 membranes. J Electrochem Soc 1993;140:1041-7.

[39] Hinatsu JT, Mizuhata M, Takenaka H. Water uptake of perfluorosulfonic acid membranes from liquid water and water vapor. J Electrochem Soc 1994;141:1493-8.

[40] Yang C, Srinivasan S, Bocarsly AB, Tulyani S, Benziger JB. A comparison of physical properties and fuel cell performance of Nafion and zirconium phosphate/Nafion composite membranes. J Membrane Science 2004;237:145-61.

[41] Husar A, Higier A, Liu H. In situ measurements of water transfer due to different mechanisms in a proton exchange membrane fuel cell. J Power Sources 2008;183:240-6.

[42] Jinnouchi R, Yamada H, Morimoto Y. Measurement of electro-osmotic drag coefficient of Nafion using a concentration cell. 14th International Conference on the Properties of Steam in Kyoto 2004;32:403-406.

[43] Olesen AC; Berning T, Kaer SK. On the diffusion coefficient of water in poylmer electrolyte membranes. ECS Transactions 2012;50(2):979-91.

[44] Motupally S, Becker AJ, Weidner JW. Diffusion of water through Nafion 115 membranes. J Electrochem Soc 2000;147:3171-7.

[45] Hussaini IS, Wang CY. Visualization and quantification of cathode channel flooding in PEM fuel cells. J Power Sources 2009;187:444-51.

[46] Perrin JC, Lyonnard S, Guillermo A, Levitz P. Water dynamics in ionomer membranes by field-cycling NMR relaxometry. Magnetic Resonance Imaging 2007;25:501-04.

[47] Mosdale R, Gebel G, Pineri M. Water profile determination in a running proton exchange membrane fuel cell using small-angle neutron scattering. J Membrane Science 1996;118:269-77.

[48] Turhan A, Kim S, Hatzell M, Mench MM. Impact of channel wall hydrophobicity on through-plane water distribution and flooding behavior in a polymer electrolyte fuel cell. Electrochimica Acta 2010;55:2734-45.

[49] Gurau V, Liu HT, Kakac S. Two-dimensional model for proton exchange membrane fuel cells. AIChE J. 1998;44:2410-22.

[50] Shimpalee S, Greenway S, Spuckler D, Van Zee JW. Predicting water and current distributions in a commercial-size PEMFC. J Power Sources 2004;135:79-87.

[51] Berning T, Djilali N.Three-dimensional computational analysis of transport phenomena in a PEM fuel cell – a parametric study. J Power Sources 2003;124:440-52.

[52] Lum KW, McGuirk JJ. Three-dimensional model of a complete polymer electrolyte membrane fuel cell – model formulation, validation and parametric studies. J Power Sources 2005;143:103-24.

[53] Liu Z, Mao Z, Wang C, Zhuge W, Zhang Y. Numerical simulation of a mini PEMFC stack. J Power Sources 2006;160:1111-21.

[54] Shimpalee S, Ohashi M, VanZee JW, Ziegler C, Stoeckmann C, Sadeler C, Hebling C. Experimental and numerical studies of portable PEMFC stack. Electrochimica Acta 2009;54:2899-911.

[55] Macedo-Valencia J, Sierra JM, Figueroa-Ramirez SJ, Diaz SE, Meza M. 3D CFD modeling of a PEM fuel cell stack. J Hydrogen Energy 2016;41:23425-33.

ABSTRACT

It is known that the peformance of proton exchange membrane (PEM) fuel cells is dependent on the water and heat management of the cell during operation. Water management dictates the ionomer membrane hydration, since high membrane water content results in high performance of the cell. The heat management is closely correlated to the water management due to the fact that the relative humidity of the reactants depends on the temperature of the reactants during operation.

Currently developed PEM fuel cells use external humidification on a regular basis to enable high membrane hydration and thereby maximize the cell efficiency. However, since the relative humidity of the reactants is high upon entry to the cell, and the cell produces additional water and heat during operation, the operating range must be limited to prevent the flooding and starvation of the cell.

This work investigates the current state of the art in PEM fuel cell research by reviewing the work of other authors, and investigates the possibility of complete removal of the external humidifiers from the PEM fuel cell system, without compromising the performance of the cell. If such system proves to be feasible, it would result in a significant reduction in PEM fuel cell system complexity and price, wider operating range, and would result in partial or complete solution of the problem of liquid water removal from the cell.

SAŽETAK

Poznato je da je učinkovitost membranskog (PEM) gorivnog članka ovisna o upravljanju vodom i toplinom prilikom rada gorivnog članka. Upravljanje vodom diktira hidrataciju ionomerne membrane, budući da je posljedica visokog sadržaja vode u membrani visoka učinkovitost gorivnog članka. Upravljanje toplinom je usko povezano sa upravljanjem vodom budući da relativna vlažnost reaktanata ovisi o temperaturi reaktanata tijekom rada.

Membranski gorivni članci koji se trenutno mogu naći na tržištu uobičajeno koriste vanjske ovlaživače na regularnoj osnovi da bi se postigla visoka hidratacija membrane, te na taj način maksimizirala učinkovitost članka. Međutim, budući da je relativna vlažnost reaktanata visoka po ulasku u gorivni članak, pri čemu gorivni članak proizvodi vodu i toplinu tijekom rada, radno područje se mora ograničiti u svrhu sprečavanja plavljenja i starvacije gorivnog članka.

U ovom radu se proučava trenutno stanje istraživanja u području membranskih gorivnih članaka pregledom radova drugih istraživača, pri čemu je naglasak na mogućnosti potpunog uklanjanja vanjskih ovlaživača iz sustava, bez kompromitiranja učinkovitosti sustava membranskih gorivnih članaka. Ukoliko je to moguće projektirati takav sustavi, rezultat bi bila značajno umanjena kompleksnost i cijena sustava, prošireno radno područje, što bi također rezultiralo u djelomičnom ili potpunom rješavanju problema uklanjanja tekuće vode iz gorivnog članka